SELENOLOGY TODAY

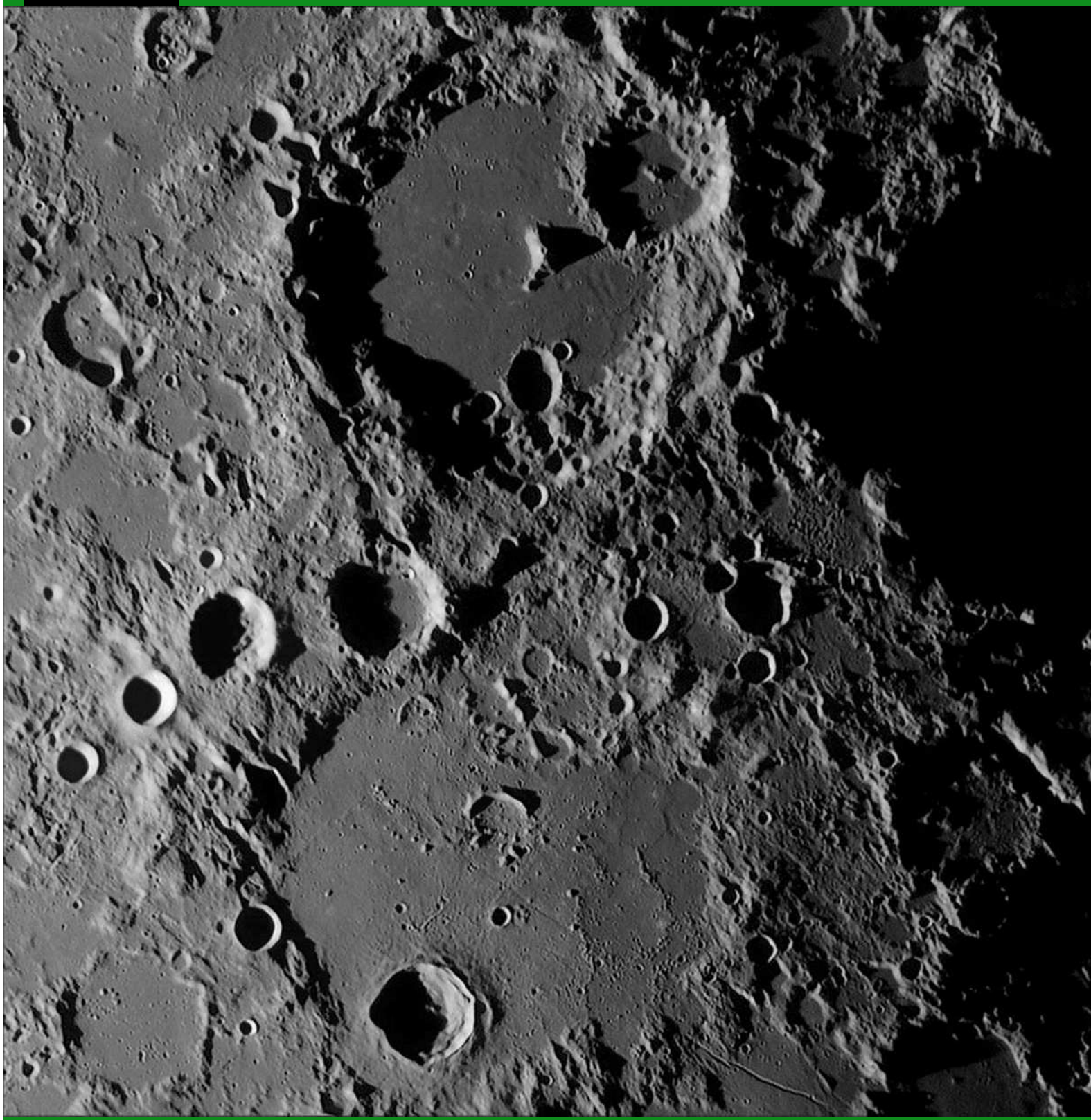

SELENOLOGY TODAY # 14
June 2009

http://www.glrgroup.eu/old/

Selenology Today is devoted to the publication of contributions in the field of lunar studies.

Manuscripts reporting the results of new research concerning the astronomy, geology, physics, chemistry and other scientific aspects of Earth's Moon are welcome.

Selenology Today publishes papers devoted exclusively to the Moon.

Reviews, historical papers and manuscripts describing observing or spacecraft instrumentation are considered.

The Selenology Today

Editorial Office

selenology_today@christian-woehler.de

Cover
Stefan Lammel

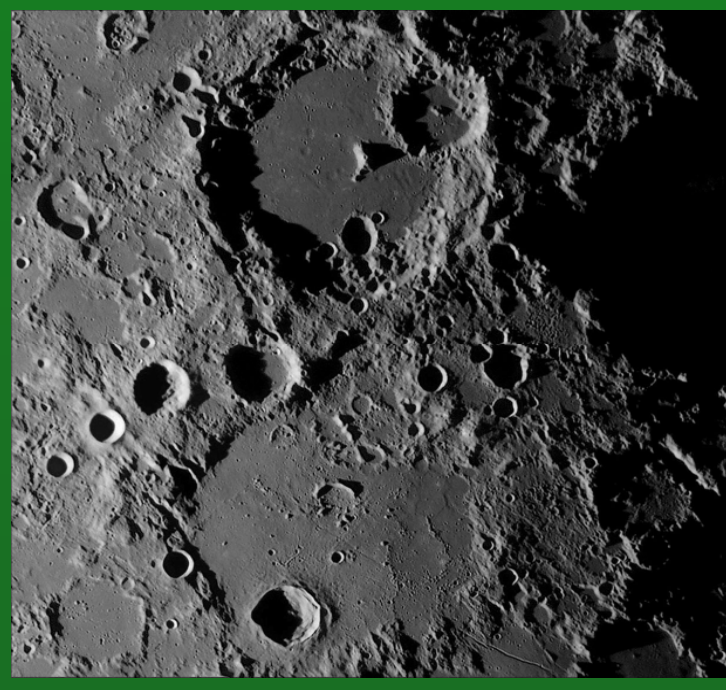

SELENOLOGY TODAY #14
June 2009

GLR group
http://www.glrgroup.eu/old/

Selenology Today website
http://digilander.libero.it/glrgroup/

Special Issue

Spectral Mapping Using Clementine UV-Visible-NIR Data Sets: Applications to Lunar Geologic Studies
By R. Evans, C. Wöhler, R. Lena……..……..1

Spectral Mapping Using Clementine UV-Visible-NIR Data Sets: Applications to Lunar Geologic Studies

Richard Evans, Christian Wöhler, Raffaello Lena
Geologic Lunar Research (GLR) Group

Abstract
This paper explores the automated production of maps of spectral parameters of lunar features using the Clementine UV-Visible-NIR data set covering the wavelength range between 415 nm and 2000 nm. Maps were produced independently using both GNU Octave and Microsoft Excel 2007. Maps were made of a) the band center minimum and depth of the principal mafic absorption trough near 1000 nm for both orthopyroxenes (890 to 945 nm) and clinopyroxenes (950 to 1000 nm); b) the band center minimum and depth of any secondary absorption feature present at higher wavelengths (1005 to 1095 nm); c) the FWHM (full width at half maximum wavelength) of the principal absorption feature; and an Optical Maturity (OMAT) map. Olivine deposits were differentiated from impact melt deposits through use of a 1500nm/2000 nm ratio image which shows olivine features as bright pixels.

Spectral properties

The Clementine lunar probe imaged the lunar surface using five UV-visible spectral bands and six near infrared bands covering the wavelength range from 415 nm to 2780 nm. The five UV-visible bands have been available on the map-a-planet website maintained by the USGS for some years. Recently, however, the first four near infrared bands covering the range from 1100 nm to 2000 nm have been calibrated so that both datasets can be used seamlessly. Calibration for the last two near infrared bands (2600 nm and 2780 nm) is generally thought to be less reliable.

Examination of wavelength vs reflectance plots made from the 415 nm to 2000 nm calibrated images provides important information about the mineral composition of the moon. Information about the identity of iron bearing (mafic) minerals (orthopyroxenes and clinopyroxenes) is contained in the band center, depth and width parameters of an absorption trough near 1000 nm. In some cases secondary absorption features due to the presence of an olivine or impact melt glass component are present at higher wavelengths. The band center, depth and width parameters of these secondary features are useful in analyzing mineral content. In addition, pyroxenes have a shallow secondary trough at about 1250 nm, however analysis of this trough was excluded from the present paper.

The continuum slope, generally taken as the slope of a line connecting the reflectance value at 750 nm and 1500 nm, is steeper for more mature (i.e. weathered) lunar features and shallower for more recent, less weathered lunar features. This slope can be used to correct the depth of the mafic absorption trough near 1000 nm for the effects of weathering by micrometeorite bombardment and long term exposure to solar radiation.

Weathering causes the absorption trough to become shallower and less deep.
The trough characteristics can be restored by dividing reflectance values by the continuum slope.
The maturity of a lunar feature on Clementine PDSMAP images (which have been calibrated to the standard Apollo 16 soil sample #62231 by the John Adams method can be mapped using the OMAT or optical maturity value where:

$$\mathbf{OMAT = [\ (R_{750} - 0.04)^2 + \ (R_{950}/R_{750} - 1.22)^2\ ]^{0.5}}$$

The PDSMAP image grayscale values are first converted to absolute reflectance by multiplying by 0.000135. OMAT values have been directly related to crater age. The larger the OMAT value, the more recent and less mature the lunar feature. In Fig. O-1 of Copernicus below, the central peak material is newer and fresher than the mare material (OMAT values of roughly 0.35 vs 0.2).

If the OMAT values of the central peaks and the adjacent mare were the same, this would have implied that the crater was the same age as the adjacent mare. Similarly, comparing Fig. O-1 and Fig. O-2, it is clear that Aristarchus is a much younger crater than Copernicus (OMAT value of 0.5 vs 0.35 for the central peak area) and that Aristarchus crater is younger than the adjacent terrain.
Copernicus is estimated to be 810 million years old.

Aristarchus is estimated to be about 450 million years old. Because of the complications in spectral interpretation introduced by the maturation process, mineralogical interpretation of spectra is sometimes confined to a particular range of OMAT values. For example, topography with an OMAT value greater than 0.3 is sometimes accepted as a threshold for the most reliable interpretation of spectra with minimal influence by the maturation process.

Fig. O-1

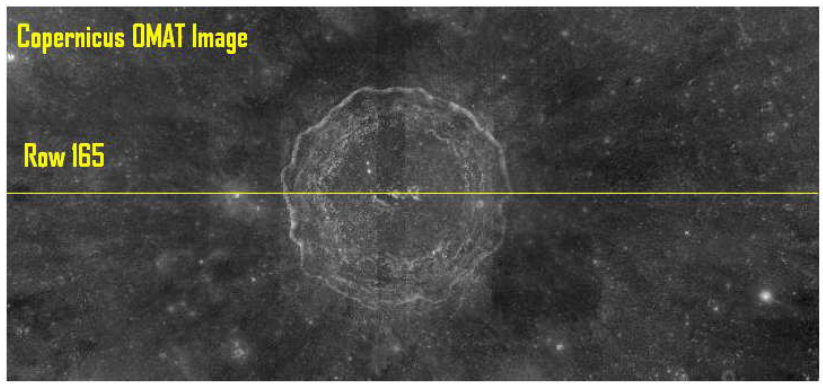
Copernicus OMAT Image
Row 165

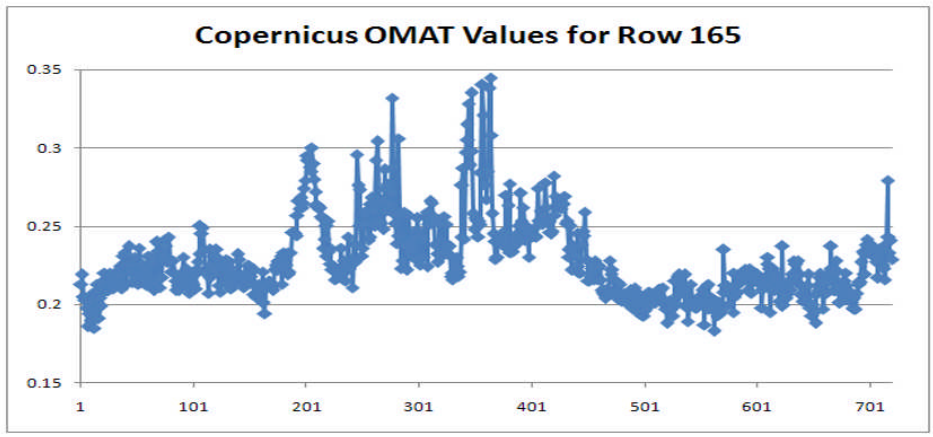
Copernicus OMAT Values for Row 165
0.35
0.3
0.25
0.2
0.15
1
101
201
301
401
501
601
701

Fig. O-2

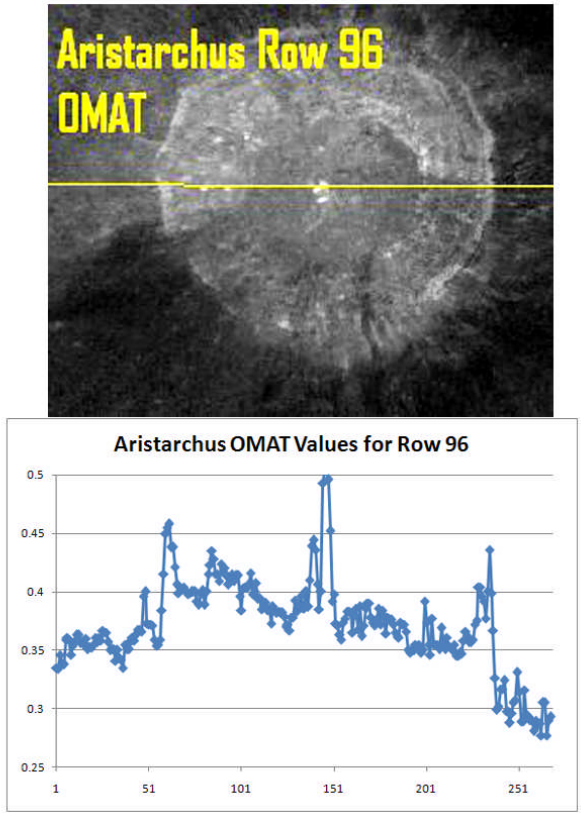

Pyroxene has an absorption band near 1000 nm. Some types of basalt have a high olivine content (up to 10 to 20 percent). The effect of high olivine levels is to broaden the pyroxene band and to move it slightly towards higher wavelengths. All rocks containing pyroxenes have bands between approximately 900 and 1000 nm. Norite, which is comprised of plagioclase feldspar and low-Ca pyroxene, has an absorption band between 900 and 930 nm. As the low-Ca pyroxene content increases, the strength of the absorption band also increases. If an area of lunar rock has an absorption band between 930 and 950 nm, it is probably noritic, but its pyroxene may have a higher Ca content, or the norite may have some high-Ca pyroxene mixed in. Gabbro rocks are very similar to basalts in mineral content, but gabbro rocks were formed intrusively while basalts were formed extrusively.

Lunar gabbros tend to have a lower pyroxene content than lunar basalts. Lunar gabbros can be almost pure high-Ca pyroxene, with an absorption band range of 970 to 1000 nm, or they can be both high-Ca and low-Ca pyroxene, with an absorption band range of 950 to 970 nm.
Dunite and troctolite, two rocks composed of olivine, have absorption bands centered beyond 1000 nm and often around 1100 nm when present in a purer form unmixed with

other minerals. Dunite is almost pure olivine, while troctolite is made up of both plagioclase feldspar and olivine. In both cases, the strength of the absorption band at 1100 nm depends on the level of olivine as compared to the level of plagioclase.
The 1-µm absorption band in olivines is due to a crystal field absorption of Fe^{2+}. "Fo" identifies forsterite (Mg_2SiO_4) in the forsterite-fayalite (Fe_2SiO_4) olivine solid solution series. The Fo 29 sample (KI3291 from King and Ridley, 1987) has an FeO content of 53.65%, while the Fo 91 sample (GDS 71; labeled Twin Sisters Peak in King and Ridley, 1987) has an FeO content of 7.93%.

The identification of the olivine composition can be done with the comparison of spectra collected from http://speclab.cr.usgs.gov/spectral.lib06/ds231/datatable.html

The 1000 nm band position varies from about 1080 nm at Fo 10 to about 1050 nm at Fo 91 (King and Ridley, 1987), corresponding to a FeO content >50 % or < 9% respectively. This comparison is useful for identification of the ferroan type in the forsterite-fayalite olivine solid solution series.

Pure anorthosite is composed almost entirely of plagioclase feldspar, and has no absorption bands in the visible and near-infrared parts of the spectrum. But the term anorthosite is used for lithologies that are at least 90 percent plagioclase feldspar and containing up to ten percent mafic (i.e. iron containing) minerals.

The mafic component can be orthopyroxene, pyroxene, olivine, or a mixture of various mafic elements. Anorthosite is a major component of the lunar crust, but areas of nearly pure plagioclase feldspar (i.e. anorthite) with little or no mafic contamination are much less common.

An illustration of the spectral differences, which in turn denote the chemical differences between specific minerals, is shown in Fig. O-3.

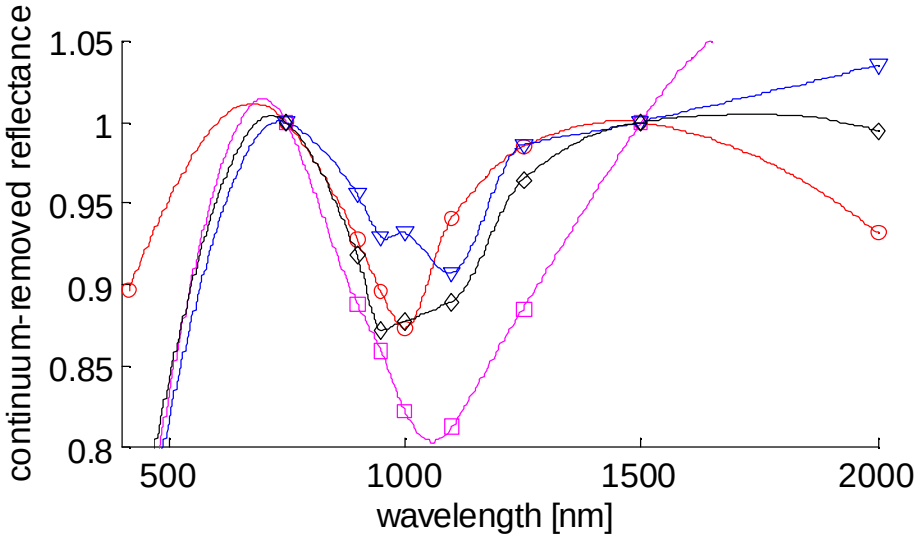

Fig. O-3: Example spectra of the Aristarchus region. Circles: pyroxene trough; triangles: double trough (pyroxene and olivine); diamonds: single trough with inflection feature (minor admixed olivine component); squares: olivine trough.

Figs. O-4 and O-5 show the diagrams with the UVVIS+NIR spectra of all Apollo landing sites and the three Luna landing sites, respectively, from which samples were brought back to Earth.

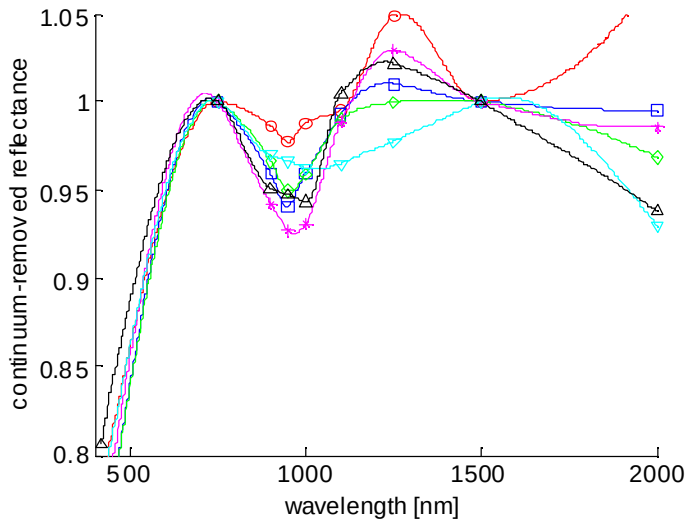

Fig. O-4 Apollo spectra. Red: Apollo 11; blue: Apollo 12; green: Apollo 14; magenta: Apollo 15; cyan:Apollo 16; black: Apollo 17.

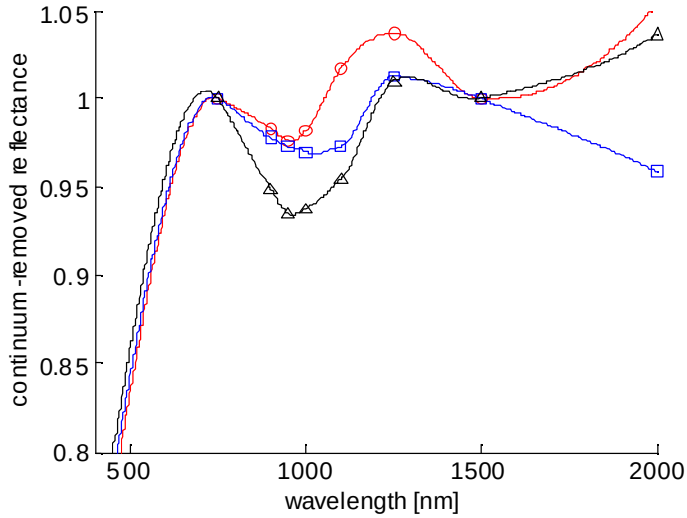

Fig. O-5 Luna spectra: Red: Luna 16; blue: Luna 20; black: Luna 24.

Methodology

Nine Clementine UV-visible and near infrared spectral bands covering the range from 415 nm to 2000 nm were downloaded in 16 bit TIFF format from the map-a-planet website maintained by the USGS (see http://www.mapaplanet.org/explorer/moon.html). A geographic area was selected and the color albedo (i.e. natural color) image was examined. The UV-visible bands 1 through 5 corresponding to 415 nm, 750 nm, 900 nm, 950 nm, and 1000 nm were requested individually in 16 bit tiff format. The database was then changed to the near infrared enhanced color database without changing the geographic location.

Near infrared bands 1 through 4 corresponding to 1100 nm, 1250 nm, 1500 nm 2000 nm were then requested individually in 16 bit tiff format. The images were then converted to image txt format using the Import function in ImageJ.

Periodically the PDSMAP website experiences problems with the downloading of 16 bit tiff images, and if this occurs then it is also possible to use 16 bit raw images which have also been completely pre-calibrated and are available on the PDSMAP website.

Subroutines were written for GNU Octave and for Microsoft Excel 2007 to extract continuum divided absorption trough parameter data from this set of image txt files and to apply an interpolation of the data points. This resulted in the automated production of maps of a) the band center minimum and depth of the principal mafic absorption trough near 1000 nm segregated into orthopyroxene (890-945 nm) and clinopyroxene (950-1000nm) troughs; b) the band center minimum and depth of any secondary absorption feature including both true troughs and curve inflections (i.e. “shoulders”) present at higher wavelengths between 1005-1095 nm; and c) the FWHM width of the principal

absorption feature.
The Microsoft Excel 2007 version employs a cubic spline interpolation routine, while the GNU Octave version is based on an Akima interpolation (Evans et al., 2009). Comparison of results showed no significant difference in band center or band depth determinations, but there was a slight non-systematic variation in FWHM widths in the results produced by the two program versions.

The automated spectral parameter mapping pursued in this paper results from a direct method of algorithm based analysis of the continuum divided spectrum as described above. A more detailed description of the Excel 2007 workbook used in the spectral mapping process is provided in Appendix I of this paper.

Previous work by Le Mouelic (2000) and Lucey (1998) involved mapping of iron and titanium content as well as the estimation of other spectral parameters including continuum slope and mafic band depth. For those that are interested, maps modelled on this work are presented in Appendix II. Appendix III contains several additional examples of lunar feature spectral maps made in Excel.

Results
Aristarchus:

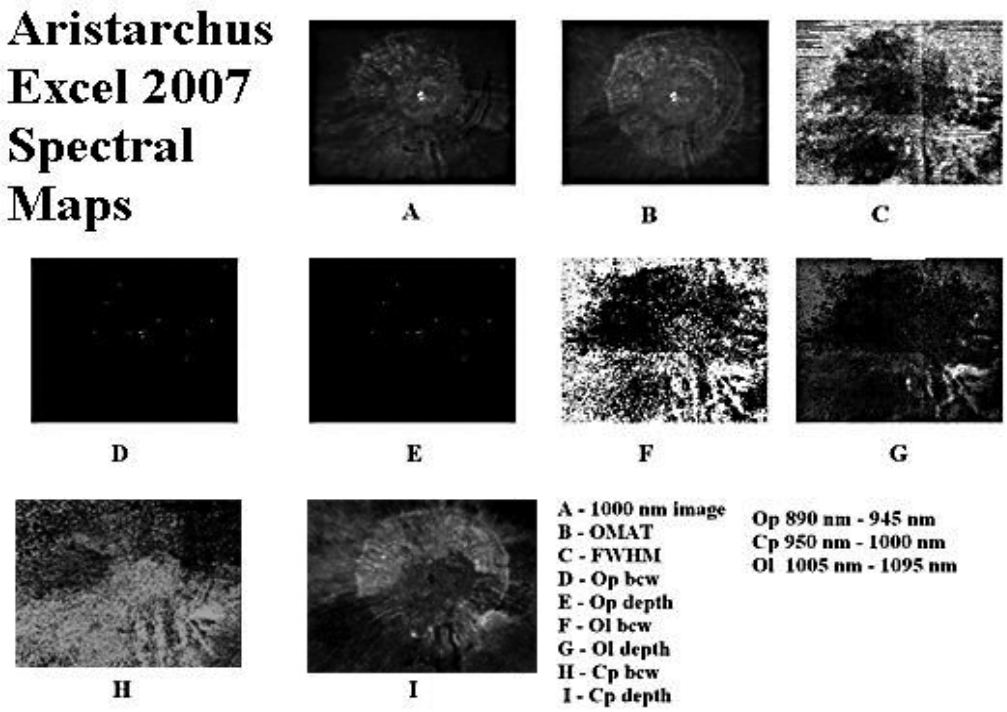

Fig. 1a

Fig. 1b

Aristarchus - Octave Maps

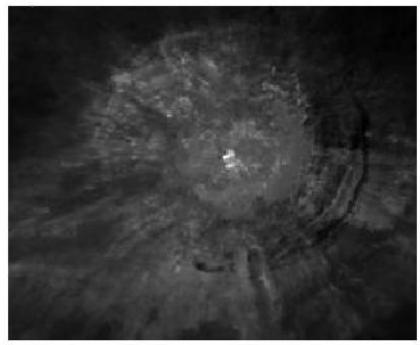

1000 nm PDSMAP

Bandcenter Map

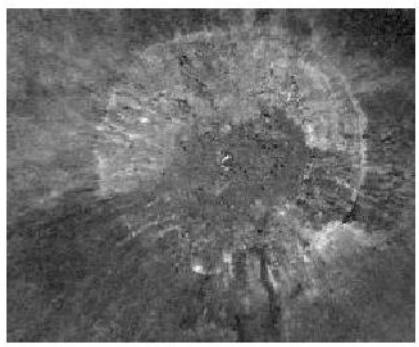

Band Depth Map

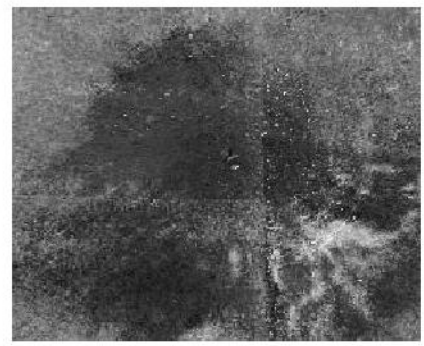

FWHM Map

Fig 1c Ratio Map 2000nm/1500nm (olivine features appear bright)

Fig 1d

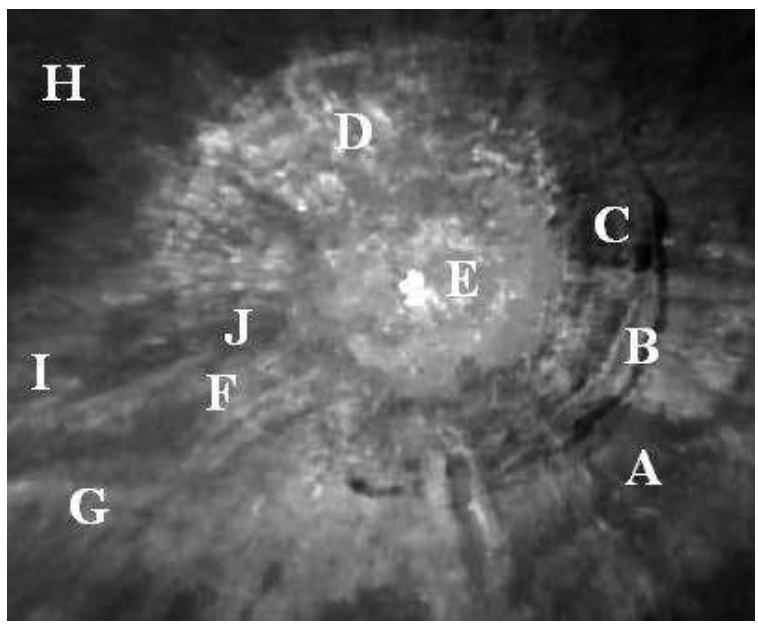

Table 1e (Refer to Fig. 1d for locations A thru J)

	Op bcw	Op depth	Cp bcw	Cp depth	Ol bcw	Ol depth	OMAT	FWHM
A	0	0.0	1.0	0.195	1.026	0.197	0.413	279
B	0	0.0	0.99	0.133	1.005	0.117	0.365	222
C	0	0.0	0.97	0.18	0	0.0	0.419	265
D	0	0.0	0.98	0.152	0	0.0	0.442	246
E	0	0.0	1.0	0.130	1.005	0.056	0.487	208
F	0	0.0	0.98	0.150	1.005	0.077	0.416	262
G	0	0.0	1.0	0.1194	1.005	0.061	0.350	228
H	0	0.0	0.97	0.146	1.025	0.120	0.374	266
I	0	0.0	0.985	0.147	0	0.0	0.414	279
J	0	0.0	0.97	0.198	1.005	0.0379	0.438	226

Interpretation of Aristarchus Map Data:

Olivine is concentrated primarily in the area just beyond the crater rim to the southwest although a very small focus of olivine rich terrain is also present just outside the crater rim area to the southeast. The possibility that the olivine bcw and depth maps identify impact melt rather than olivine is excluded by the 2000nm/1500nm ratio maps which shows these foci as being bright. The remainder of the crater shows various concentrations of clinopyroxene ranging from anorthositic gabbro to gabbro and essentially no orthopyroxene is present. Olivine in mare material to the northwest of the crater indicates the presence of basalt containing a moderate amount of olivine material.

Bullialdus:
Fig. 2a

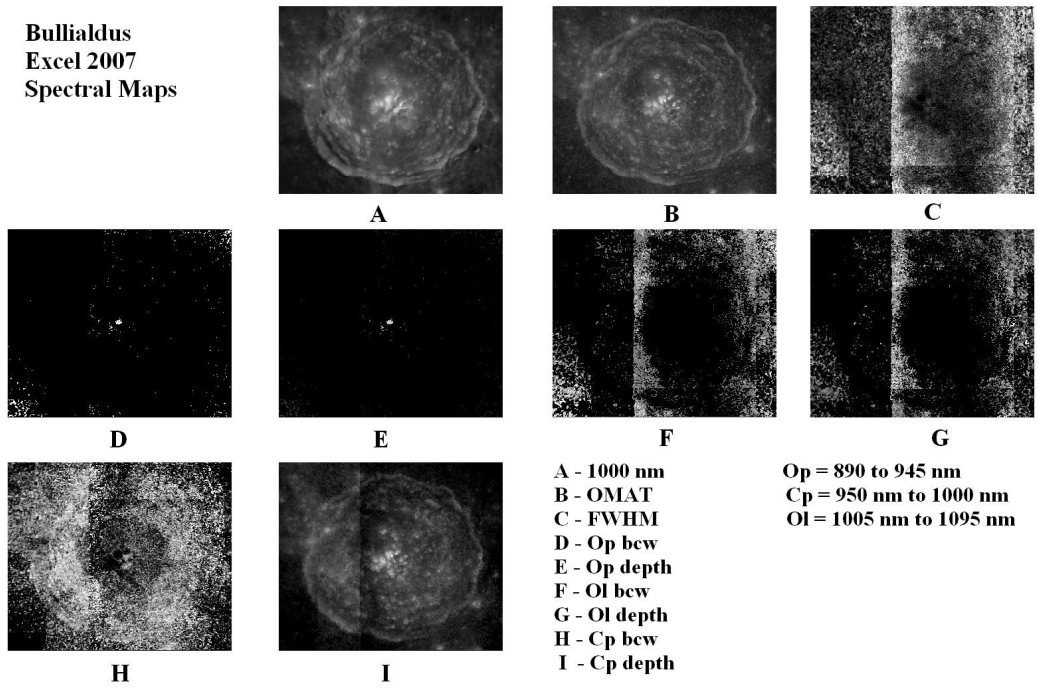

Fig. 2b
Bullialdus Central Peak Area (Enlarged)

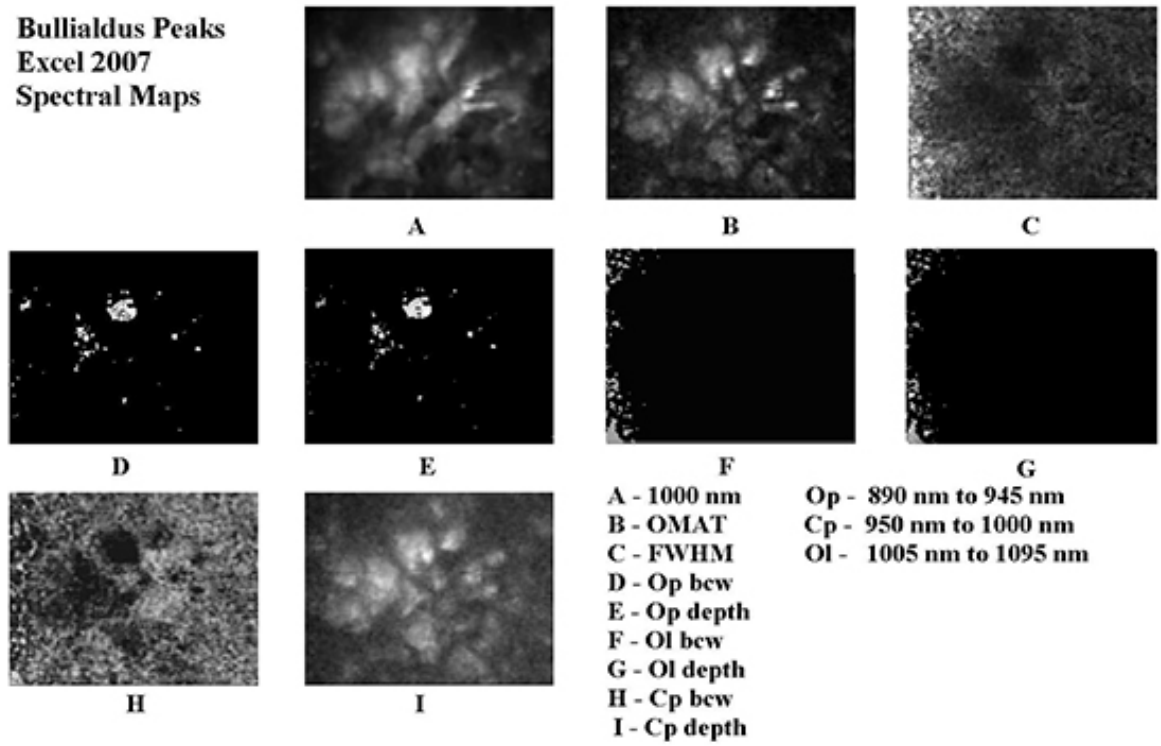

Fig. 2c

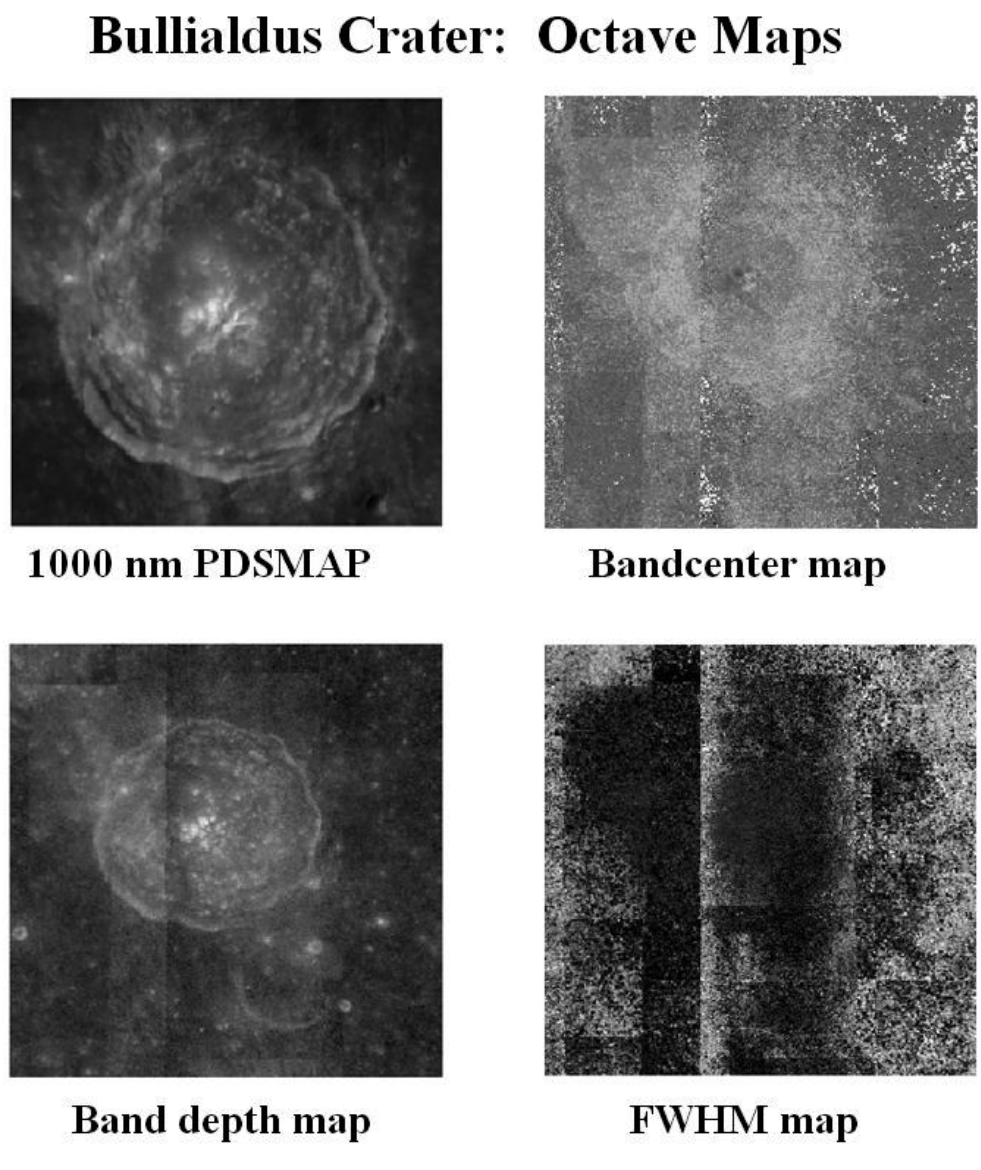
Bullialdus Crater: Octave Maps
1000 nm PDSMAP
Bandcenter map
Band depth map
FWHM map

Fig. 2d

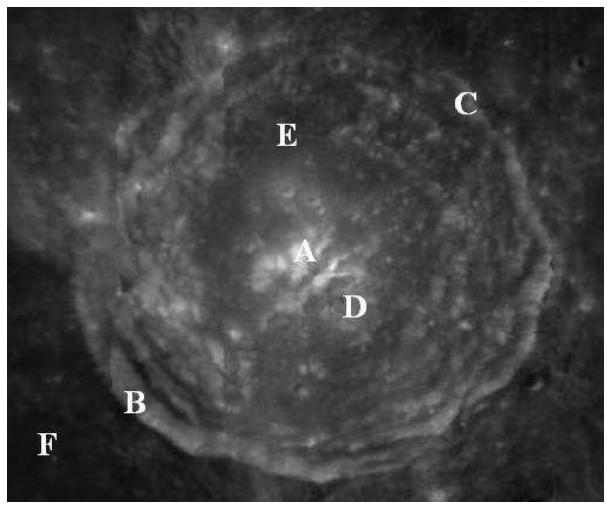

Table 2-e (Refer to Fig. 2d for locations of A thru F)

	Op bcw	Op depth	Cp bcw	Cp depth	Ol bcw	Ol depth	OMAT	FWHM
A	0.930	0.195	0.950	0.218	0	0.0	0.383	203
B	0	0.0	0.980	0.107	0	0.0	0.249	204
C	0	0.0	0.985	0.129	0	0.0	0.235	204
D	0	0.0	0.980	0.141	0	0.0	0.270	200
E	0	0.0	0.960	0.081	0	0.0	0.219	210
F	0	0.0	0.950	0.062	1.021	0.035	0.218	247

Interpretation of Bullialdus Map Data:

The central peak at location A is rich in orthopyroxenes but also contains some clinopyroxene which is also identified in the remaining central peaks within the crater. The crater rim is rich in clinopyroxenes and essentially no orthopyroxenes are identified in the rim area.

Copernicus:

Fig. 3a

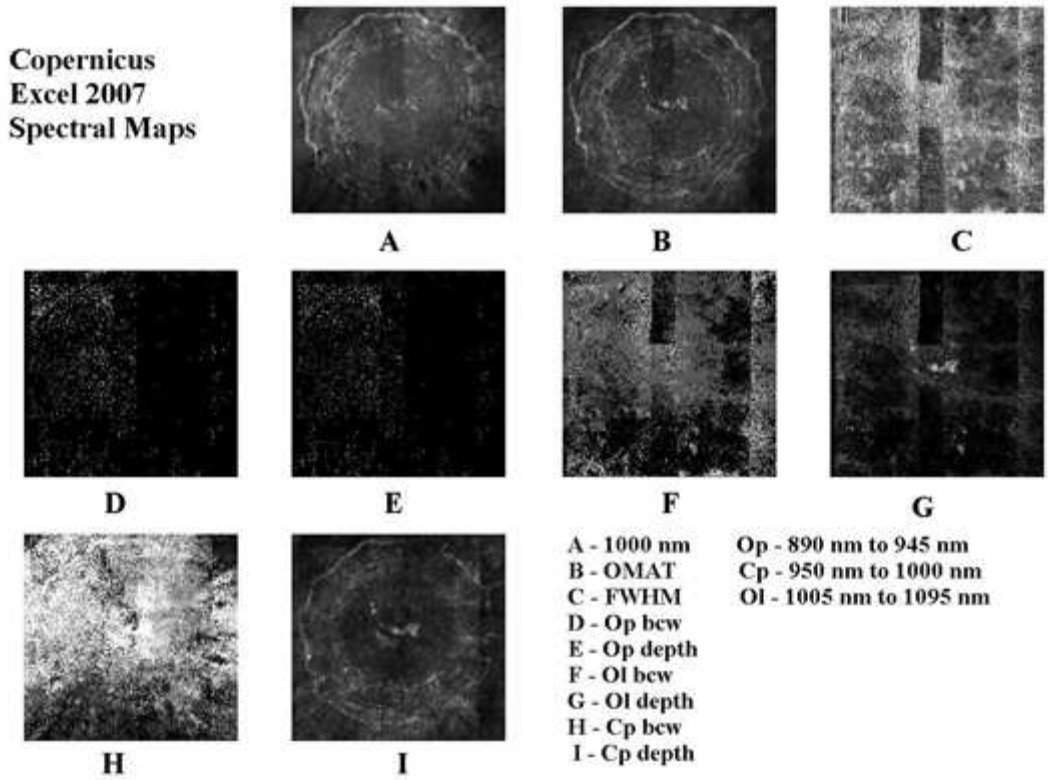

Fig. 3b

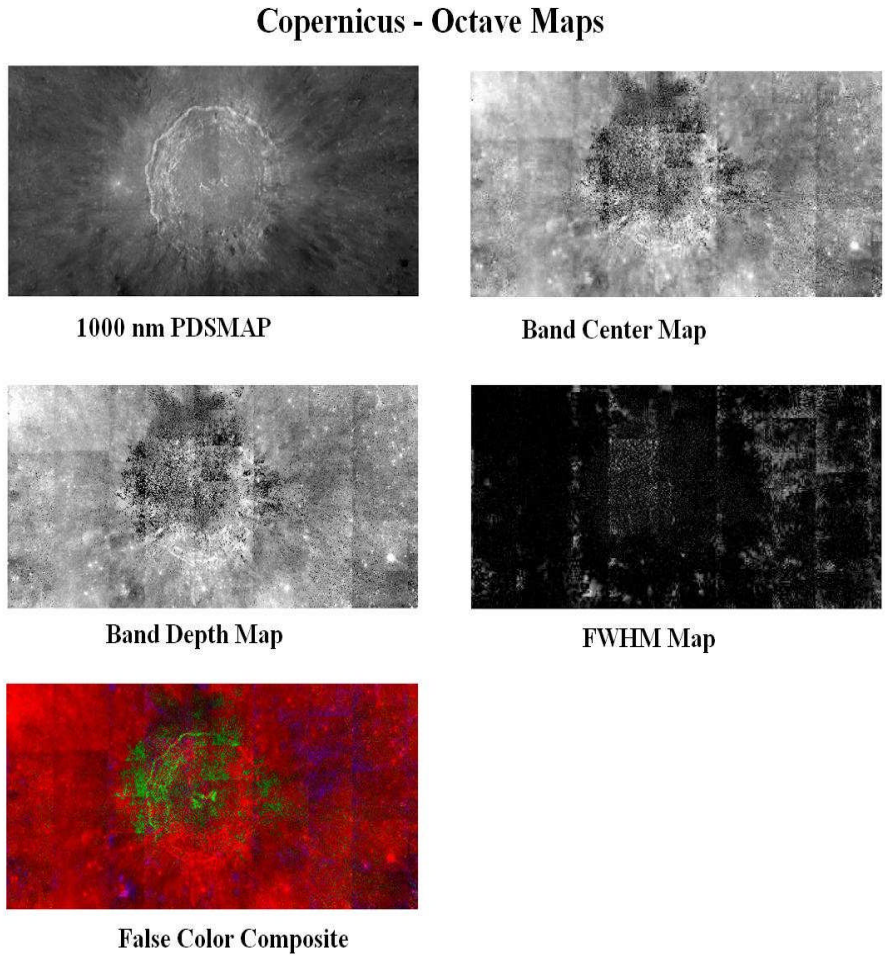
Copernicus - Octave Maps
1000 nm PDSMAP
Band Center Map
Band Depth Map
FWHM Map
False Color Composite

Fig. 3c

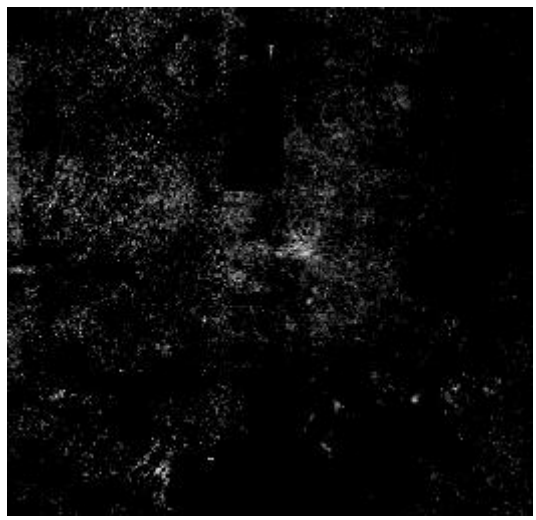

Fig. 3d

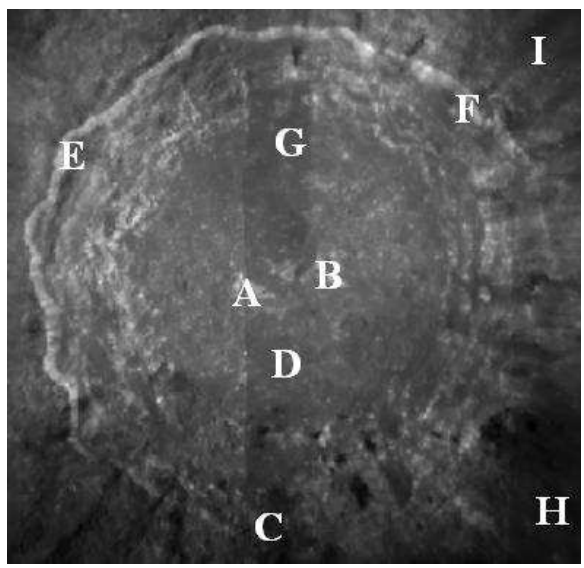

Fig. 3e (Refer to Fig. 3d for location of A thru I)

	Op bcw	Op depth	Cp bcw	Cp depth	Ol bcw	Ol depth	OMAT	FWHM
A	0	0.0	1.0	0.104	1.03	0.105	0.311	256
B	0	0.0	1.0	0.135	1.015	0.090	0.312	253
C	0	0.0	0.97	0.089	0.0	0.0	0.244	240
D	0	0.0	0.99	0.037	1.01	0.045	0.228	211
E	0	0.0	1.0	0.073	1.005	0.019	0.244	200
F	0	0.0	0.98	0.075	1.005	0.038	0.313	239
G	0	0.0	0.96	0.057	1.005	0.020	0.244	234
H	0	0.0	0.97	0.044	0.0	0.0	0.193	257
I	0	0.0	0.96	0.060	0.0	0.0	0.212	194

Interpretation of Copernicus Map Data:

The central peaks of Copernicus contain a significant amount of olivine (troctolite).

The fact that olivine rather than impact melt is identified by the olivine bcw and depth maps is confirmed by the 2000nm/1500nm ratio map which shows the central peaks as being bright.
The crater rim is mainly composed of various concentrations of clinopyroxenes, but the main constituent appears to be gabbro although small foci of orthopyroxene and olivine may also be present.

Discussion:

This paper describes a fully automated process for the mapping of specific absorption trough characteristics using Clementine UVVIS/NIR data. The band center minimum and band depth near 1000 nm subdivided into orthopyroxene and clinopyroxene band minima maps and maps of secondary troughs/shoulders at higher wavelengths, together with the FWHM width are useful in lunar mineral characterization and optical maturity maps (OMAT). Trough parameter maps were generated through the independent use of GNU Octave and Microsoft Excel 2007. These maps provide a good indication of mineral content over an extended geographic area. The Excel maps cover discrete wavelength ranges typical for orthopyroxene, clinopyroxene and olivine content.
It should be noted that neither the band center nor the trough depth alone is sufficient to interpret the local mineral composition. For example, a pixel representing an area with an absorption band center at 1020 nm might represent ferroan anorthosite if the band depth is below 5%, but might represent troctolite if the band depth is greater than 5%. The FWHM value is also useful in interpretation since larger FWHM widths favor impact melt or olivine content. The full range maps produced in GNU Octave and Excel 2007 are useful for a comprehensive interpretation of mineral content.

Editorial Note: Readers interested in working directly with a sample Excel Workbook may request one from the Selenology Today Editorial Board.

Appendix I

A1-1 to A1-3 Screen shots of Excel 2007 workbook

Table A2-1 Maps created in worksheets 13 through 18

A3-1 Band center map

A3-2 Band depth map

A3-3 FWHM map

A3-4 False color map

Appendix II

A4.1 Aristarchus Image Group:
- a Map of continuum slope
- b Map of band depth

c Map of band depth corrected for continuum slope
d Theta angle value map for titanium
e Map of titanium oxide
f Map of total iron wt %
g Map of total iron wt% as color gradient
h False color composite image of olivine deposits
i Absorption trough minimum map -Octave
j Absorption trough depth map - Octave
k FWHM map - Octave
l Key to geography of features in Table 4.1-1
m Clementine 9 band UVVIS-NIR spectra
n 5 band UVVIS spectra for olivine deposit
o 5 band UVVIS spectra for crater floor
p False color image of crater
q False color composite image of crater
r False color image of crater
(red: inv trough minima map, green: FWHM map, blue: trough minima map). Topography: band depth map.

A4.2 Alphonsus Image Group:
a Map of continuum slope
b Map of band depth
c Map of band depth corrected for continuum slope
d Map of Theta for titanium
e Map of titanium oxide wt %
f Map of titanium oxide wt%, color gradient
g Map of total iron wt %
h Map of total iron wt %, color gradient
i Map of absorption trough minimum - Octave
j Map of absorption trough depth - Octave
k FWHM map - Octave
l Excel Maps
m Key to Geography of Table 4.2 – 1
n Clementine 5 band UVVIS spectra of Alphonsus Region
o Clementine 9 band UVVIS-NIR spectra of Alphonsus dark halo crater
p False color comosite map
q False color map (red: inverted absorption trough minima map, green: FWHM map, blue: absorption trough minima map) Topography: band depth map

A4.3 Bullialdus Image Group:
a Map of continuum slope
b Map of band depth
c Map of band depth corrected for continuum slope
d Map of Theta for titanium

e Map of titanium oxide wt %
f Map of titanium oxide wt %, color gradient
g Map of total iron wt %
h Map of total iron wt %, color gradient
i Absorption trough minimum map
j Absorption trough depth map
k FWHM map
l Key to geography of features in Table 4.5-1
m False color composite map
n False color map (red: inverted trough minima map, green: FWHM map, blue: trough minima map). Topography: band depth map

Appendix III

A5.1 Excel Maps of Dionysius
A5.2 Orientation image of Dionysius
A5.3 Table of Values

References

1. Cahill, JT and Lucey PG (2007) Radiative transfer modeling of lunar spectral classes and relationship to lunar samples. J Geophysical Research Vol. 112, 23 pages.

2. Evans, R., Wöhler, C., Lena, R., 2009. Analysis of absorption trough features using Clementine UVVIS+NIR imagery. Lunar Planet. Sci. XL, abstract #1093.

3.Grier JA, McEwen AS, Lucey PG et al. (1999) Relative ages of large rayed lunar craters – Implications. Lunar and Planetary Science Conference XXX

4. Heather DJ and Dunkin SK (2003) Geology and Stratigraphy of King Crater, lunar farside. Icarus 163 pp. 307-329.

5. King TV, Ridley WI (1987) Relation of the spectroscopic reflectance of olivine to mineral chemistry and some remote sensing implications. J. Geophys. Res. 11, 457-11, 469.

6. Le Mouelic S, Langevin Y, and Erard S (2000) Discrimination between maturity and composition of lunar soils from integrated Clementine UV-visible/near-infrared data: Application to the Aristarchus Plateau. J Geophysical Research Vol 105 No E4 pages 9445-9455.

7. Lucey PG, Blewett DT and Hawke BR (1998) Mapping the FeO and TiO_2 content of the lunar swurface with multispectral imagery. J. Geophysical Research Vol. 103 No. E2 pages 3679-3699.

8. Lucey PG, Taylor JG and Hawke BR (1998) Global Imaging of Maturity: Results from Clementine and Lunar Sample Studies. Lunar and Planetary Science XXIX.

9. Sunshine JM and Tompkins S (2001) Yet another look at Copernicus: Projecting telescopic spectra onto Clementine multispectral images through spectral mixture analysis. Lunar and Planetary Science XXXII.

10. Tompkins, S. (1998) Mafic Plutons in the Lunar Highland Crust. Lunar and Planetary Science XXIX, pp. 999-1000.

11. Tompkins, S and Pieters, CM (1997) Composition of the Lunar Crust Beneath the Megaregolith. Lunar and Planetary Science XXVIII, LPI, Houston, TX 1439-1440.

12. van der Bogert, CH and Schultz, PH (2002) King crater impact melt compositions: Possible impactor contamination. Lunar and Planetary Science Conference XXXIII.

Appendix I: Description of Microsoft 2007 Mapping Workbook

Absorption trough minimum, band depth, OMAT and FWHM maps shown in the paper were created using GNU Octave (http://www.gnu.org/software/octave/) or Microsoft Excel 2007. Octave provides a rapid and efficient means of generating absorption trough maps, but most amateur astronomers are probably unfamiliar with this program. On the other hand, Excel is a commonly available and widely used program. Many if not most amateur astronomers are probably familiar with Excel. Map creation can be performed using Excel using a visual basic application (VBA) program with several subroutines, for each map type, however it is necessary to expand the function library of Excel to include a 3rd order spline fit function for data point interpolation and also a function to render a curve segment as a polynomial equation. This is done by using the Add-in capability of Excel as described below.

Excel workbook templates and required Excel function expansion "Add-ins"for trough parameter mapping:

The Excel 2007 workbooks requires a free Excel add-in function library which is available at no cost from xlxtrfun.com is available from: http://www.xlxtrfun.com/XlXtrFun/XlXtrFun.htm. The spline function is added to the engineering function library of Excel via a very simple procedure described at this link. It simply involves copying a single .xll file to the XLSTART folder. A basic description of the method of map generation is described below and a discussion of how to generalize the workbooks to enable the calculation of maps of other lunar features is provided. The spline fit is used

by all of the workbooks and is required for map creation. The workbook requires a second Excel add-in function (trilookup) which is available at nominal cost from www.trimill.com . It provides the best fit polynomial function to a curve segment and is incorporated into the workbook in the same way.

Basic Worksheet Layout and Calculations:

The Excel 2007 workbooks input Clementine spectral maps between 415 nm and 2000 nm and output band center and band depth maps for orthopyroxenes (890 nm to 945 nm), clinopyroxenes (950 nm to 1000 nm), olivines/impact melt features (1005 nm to 1095 nm), an optical maturity map (i.e. OMAT), and a FWHM map of the lunar feature of interest. The clinopyroxene band center and band depth maps are created in worksheets 13 and 14 respectively. The olivine band center and band depth maps are created in worksheets 16 and 17 respectively. The FWHM map is created in worksheet 15. The OMAT map is created in worksheet 18. The orthopyroxene band depth and band center maps are created in worksheets 19 and 20 respectively.

Loaded Clementine Data into the Workbooks:

- ImageJ used to prepare Clementine 9 band image sets for import into Excel worksheets

Using the free program ImageJ (available here: http://rsbweb.nih.gov/ij/), Clementine nine band image sets of any lunar geography can be cropped and converted to 32 bit txt format for import into the Excel workbooks. If desired, image sets can be re-scaled in Image J. This is done using the Image>Scale menu in ImageJ while working with an imported image series (see below).

Cropped versions of the Clementine nine band data set in 16 bit tiff format (from 415 nm to 2000 nm) are usually used because they require less time to calculate than uncropped data. Clementine images are imported into ImageJ as an image sequence, the images are cropped to best advantage, and the image sequence is saved as as individual 32 bit txt files whose names preserve their wavelength band identity. To do this, the Files>Import>Image Sequence menu is used to bring the Clementine 16 bit tiff image set into ImageJ for cropping. The Clementine nine band image set in 16 bit tiff format should be named according to band wavelength (i.e. 415.tif, 750.tif, 900.tif etc.). They should be the only files present in the folder in which they reside. It is only necessary to click on the first file in the Open Image Sequence menu to import the entire image sequence. After simultaneous cropping of all images in the series by boxing the area desired and applying the crop function (thus preserving their relative alignment to each other), the resulting cropped image files are then resized if this is advantageous. Resizing, if desired, is done using the Image>Scale menu in ImageJ. For example for

Excel 2007 the pixel size could be set at 293 rows by 236 columns. The image series is then saved as an image sequence using File>SaveAs>Image Sequence menu. Files must be saved in 32 bit txt format with the individual file names preserved as the image slice names. It is very important that the images be imported into the Excel worksheets 1 through 9 in the correct band order (i.e. 415, 750, 900, 950, 1000, 1100, 1250, 1500, and 2000 nm) with 415 nm in worksheet 1, the 750 nm image in worksheet 2, the 900 nm image in worksheet 3 etc., until the 2000 nm image is copied to worksheet 9. All txt files should be copied to worksheets starting at the row 1 and column 1 position.

Worksheet 10: The Calculating and Mapping Area of the Workbook

Worksheet 10 is the basic work and calculation area of the workbook. Mapping calculations are done here and the absorption trough minimum map is created here. **It is essential that the total number of rows and columns be intered into cells L3 and L4 respectively of worksheet 10.** The first 9 columns of worksheet 10 hold the Clementine 9 band data set for a single pixel per row. The data is sequentially located from 415 nm to 2000 nm in columns A thru I respectively.

Columns M through S use formulas to calculate the continuum divided reflectance spectrum where the continuum line is placed at 750 nm and 1500 nm, and the data set for continuum division is provided by the same row of columns A thru I. Columns T, U and V calculate the OMAT value for each map pixel. For the lunar feature of interest, the continuum line divided results are loaded for all rows. As long as the total number of rows and columns into cells L3 and L4 of worksheet 10 as described above, the program will automatically initialize for a new data set that has been substituted into worksheets 1 through 9 in place of the loaded image set of interest. The usual continuum line is placed at 750 nm and 1500 nm, but this can be varied if necessary. Occasionally it may be advantageous to use a 750 nm to 2000 nm continuum line. The OMAT map is created in worksheet 18. Worksheets 19 and 20 contain the orthopyroxene band depth and band center maps respectively.

The maps are created either clicking on the Command Button present within worksheet 10 or alternately by pressing and holding the control key and pressing the f key. The spectral parameter maps will be generated in image reverse column order in worksheets 13 through 18. The maps will take longer or shorter to create depending on the row by column size of the data image set in worksheets 1 through 9. Finished maps can be copied by selecting all map columns and using the Excel copy command. A finished txt map generated in worksheet 13 through 18 can then be exported from Excel as an MS-dos txt file. This is doing using the SaveAs command in the Excel menu. The finished maps can then be imported into ImageJ as a txt image and can be examined and horizontally reversed using the Image>Rotate menu in ImageJ.

Workbook Screenshots Explained:

Screen shots of Worksheet 10 are shown in the Figures below. For illustrative purposes, the workbook shown in Figures A-1 through A-3 uses the 9 band Clementine UVVIS/

NIR dataset for Copernicus. Note again that the total number of rows must be entered into cell L3 and the total number of columns must be entered into cell L4 before calculation of the map can begin. In Fig. A-1, the first Row shows wavelength information. Clementine nine band data can be seen in Columns A through I, beginning with Row 2 and continuing downward for other pixels in the same image column, starting at Row 2 and continuing downwards. Continuum line calculations are present in Columns J and K. Columns M through S show the continuum divided result for Columns B through H. General information about the worksheet and the control button for beginning map creation are shown in Column L. OMAT calculations for each map pixel in the data column under analysis are shown in columns T through V.

Screen Shots of Excel Workbook for Absorption Trough Minima Calculation

Fig. A1-1

	A	B	C	D	E	F	G	H	I	J	K	L	M	N	O	P	Q	R	S	T	U	V
1	415	750	900	950	1000	1100	1250	1500	2000	slope	y interce	X1	750	900	950	1000	1100	1250	1500			OMAT
2	621	1008	1038	1043	1080	1135	1215	1343	1510	0.44667	673	Y1	1	0.96558	0.95049	0.96457	0.97481	0.98674	1	0.00096	0.03433	0.18784
3	625	1018	1042	1056	1080	1117	1220	1334	1505	0.42133	702	721	1	0.96374	0.95803	0.96142	0.95841	0.99295	1	0.00095	0.03337	0.18526
4	633	1029	1059	1065	1089	1138	1229	1357	1515	0.43733	701	331	1	0.96748	0.9539	0.95666	0.96272	0.98504	1	0.00094	0.03423	0.18755
5	610	996	1026	1024	1062	1117	1190	1325	1496	0.43867	667	Enter Total Rows in Cell L3	1	0.96628	0.94488	0.96051	0.9717	0.97916	1	0.00096	0.03682	0.19438
6	617	1004	1036	1036	1065	1128	1192	1316	1471	0.416	692	Enter Total Columns in Cell L4	1	0.97149	0.95291	0.96119	0.98121	0.9835	1	0.00096	0.03539	0.19066
7	636	1064	1092	1079	1118	1186	1296	1394	1608	0.44	734		1	0.96637	0.93663	0.9523	0.97373	1.00935	1	0.00093	0.0424	0.20814
8	636	1046	1087	1092	1114	1212	1295	1405	1589	0.47867	687	CREATE MAP	1	0.97245	0.95644	0.95568	0.99874	1.00752	1	0.00094	0.03098	0.17866
9	631	1049	1081	1087	1098	1180	1290	1397	1606	0.464	701		1	0.96639	0.95201	0.94249	0.97408	1.00703	1	0.00093	0.03377	0.1863
10	631	1028	1062	1061	1085	1170	1275	1411	1585	0.51067	645		1	0.96143	0.93883	0.93885	0.96956	0.99351	1	0.00095	0.03531	0.1904
11	629	1025	1059	1062	1076	1161	1248	1357	1568	0.44267	693		1	0.97031	0.95372	0.94746	0.98395	1.00134	1	0.00095	0.03382	0.18646
12	639	1070	1086	1083	1123	1167	1265	1388	1577	0.424	752	Pre-loaded data:	1	0.95801	0.93782	0.95493	0.95781	0.98674	1	0.00092	0.0432	0.21006
13	642	1069	1085	1084	1107	1187	1283	1392	1590	0.43067	746	Copernicus pre-loaded	1	0.95713	0.93842	0.94079	0.97316	0.99896	1	0.00092	0.04242	0.2082
14	659	1075	1091	1099	1133	1200	1296	1410	1611	0.44667	740	Worksheets 1 to 9	1	0.95534	0.94389	0.95478	0.97455	0.9982	1	0.00092	0.03908	0.19999
15	668	1077	1097	1107	1131	1209	1318	1418	1592	0.45467	736	for Copernicus	1	0.95791	0.94783	0.94989	0.97805	1.01048	1	0.00092	0.03692	0.19452
16	654	1080	1094	1098	1116	1206	1308	1432	1610	0.46933	728	full size and resolution	1	0.95097	0.93537	0.93207	0.96925	0.99493	1	0.00092	0.04134	0.20558
17	658	1076	1077	1072	1102	1184	1308	1403	1603	0.436	749	720 rows x 331 columns	1	0.94358	0.9216	0.92996	0.9637	1.01082	1	0.00092	0.05005	0.22576
18	646	1060	1068	1078	1095	1199	1280	1373	1570	0.41733	747		1	0.95136	0.94275	0.94045	0.99414	1.00893	1	0.00093	0.04122	0.20529
19	636	1045	1055	1069	1096	1158	1265	1389	1564	0.45867	701	KeyBoard Shortcut List:	1	0.94721	0.94041	0.9451	0.96057	0.99268	1	0.00094	0.03882	0.19939
20	643	1045	1064	1062	1086	1175	1255	1366	1558	0.428	724	Ctrl i - re-set after program	1	0.95925	0.93932	0.94271	0.98343	0.99682	1	0.00094	0.04151	0.20602
21	662	1066	1081	1071	1110	1197	1297	1363	1575	0.396	769	Ctrl m - load data for next c	1	0.96055	0.93521	0.95279	0.99369	1.02611	1	0.00092	0.04636	0.21745
22	662	1094	1100	1098	1127	1173	1281	1415	1558	0.428	773	Ctrl h - recalculate Cols. M t	1	0.94975	0.93082	0.93838	0.94308	0.97936	1	0.00091	0.0468	0.21844
23	618	1015	1022	1029	1054	1124	1228	1336	1514	0.428	694	Ctrl g - Delete Column A fro	1	0.947	0.93494	0.93939	0.96497	0.99919	1	0.00095	0.04252	0.2085
24	613	1013	1035	1033	1071	1125	1231	1333	1506	0.42667	693	Ctrl b - Map column presen	1	0.961	0.94052	0.95653	0.96788	1.00381	1	0.00095	0.0401	0.20262
25	607	1016	1029	1028	1058	1130	1214	1315	1504	0.39867	717	Ctrk k - Get Trough Minimur	1	0.9565	0.93818	0.94831	0.9779	0.9989	1	0.00095	0.04334	0.21046
26	605	980	1022	1006	1041	1106	1206	1299	1508	0.42533	661	Ctrl a - Repopulate AA to DI	1	0.97911	0.94454	0.95827	0.97974	1.01118	1	0.00097	0.03743	0.19597
27	609	992	1015	1018	1036	1108	1213	1300	1517	0.41067	684	Ctrl f - Create Entire Map	1	0.96336	0.94774	0.94641	0.97558	1.01308	1	0.00097	0.03755	0.19627
28	612	1022	1027	1016	1051	1137	1219	1328	1529	0.408	716	Ctrl y - repopulate formulas	1	0.94812	0.92062	0.93505	0.97613	0.99429	1	0.00095	0.05102	0.22796
29	616	997	1026	1025	1051	1148	1216	1317	1521	0.42667	677	Notes: Sheets 1 thru 9	1	0.96701	0.94703	0.95228	1.00145	1.00468	1	0.00096	0.03683	0.19441
30	610	994	1021	1013	1053	1106	1204	1311	1488	0.42267	677	hold Clementine maps crop	1	0.96558	0.93924	0.95756	0.96853	0.99889	1	0.00096	0.04035	0.20327
31	610	993	1030	1027	1057	1135	1231	1330	1515	0.44933	656	to 293 x 235 size with the 4	1	0.97133	0.94841	0.95627	0.98673	1.01095	1	0.00096	0.03451	0.18834
32	622	1005	1050	1041	1073	1133	1231	1327	1537	0.42933	683	map in Sheet 1 and the 200	1	0.98186	0.95429	0.96464	0.98073	1.00929	1	0.00096	0.03392	0.18676
33	632	1037	1065	1061	1096	1151	1246	1371	1547	0.44533	703	map in sheet 9 respectively	1	0.96485	0.94222	0.95443	0.9649	0.98915	1	0.00094	0.03875	0.19923

Fig. A1-2 shows a portion of the 105 data elements that extend from Column AA to Column DC. These cells contain the cubic spline interpolation for the calculation of specific wavelengths from 750 nm to 1500 nm. The range from 860 nm to 1250 nm is covered in 5 nm increments. The wavelength is shown in Row 1 and the interpolated trough value is shown in Row 2. The lowest value in Row 2 between AA and DC is the overall trough minimum shown in Cell AA3. The reflectance value of the trough minimum for orthopyroxene (890 nm to 945 nm) and clinopyroxene (950 to 1000 nm) is

shown in Cells AA5 and AA6 respectively. Cell AA4 shows the value of any positive slope to the curve between 1005 and 1095 nm which most closely approaches zero. This latter method is designed to detect olivine "shoulders" or significant curve inflections associated with olivine even if a well developed trough is not present.

Fig. A1-2

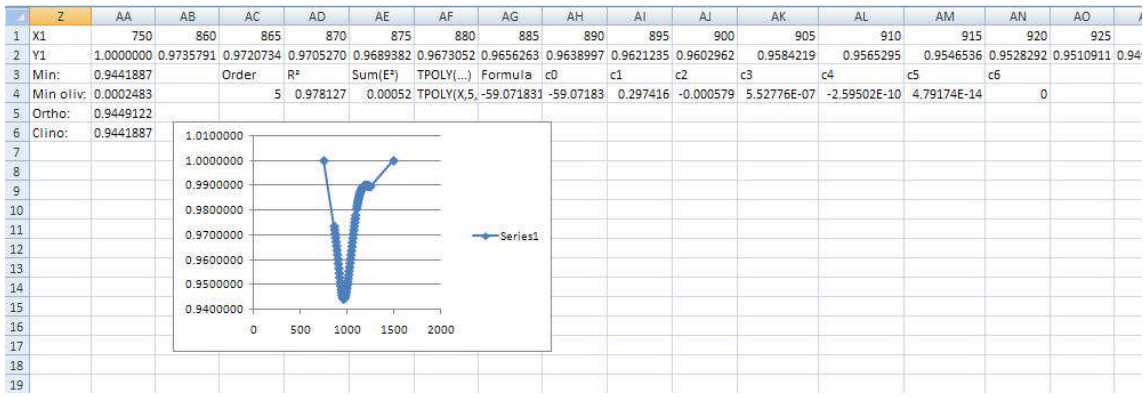

	Z	AA	AB	AC	AD	AE	AF	AG	AH	AI	AJ	AK	AL	AM	AN	AO
1	X1	750	860	865	870	875	880	885	890	895	900	905	910	915	920	925
2	Y1	1.0000000	0.9735791	0.9720734	0.9705270	0.9689382	0.9673052	0.9656263	0.9638997	0.9621235	0.9602962	0.9584219	0.9565295	0.9546536	0.9528292	0.9510911
3	Min:	0.9441887		Order	R²	Sum(E²)	TPOLY(...)	Formula	c0	c1	c2	c3	c4	c5	c6	
4	Min oliv:	0.0002483		5	0.978127	0.00052	TPOLY(X,5,	-59.071831	-59.07183	0.297416	-0.000579	5.52776E-07	-2.59502E-10	4.79174E-14	0	
5	Ortho:	0.9449122														
6	Clino:	0.9441887														

As shown in the graph in Fig. A-2 shows the absorption trough has a complex shape with a shoulder present and is fitted to a 5th order polynomial in cells AH to AM.

Fig. A1-3

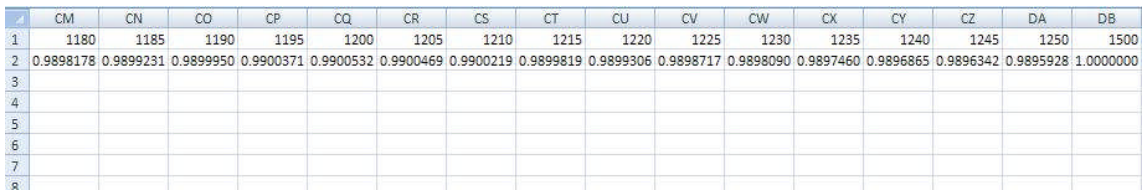

	CM	CN	CO	CP	CQ	CR	CS	CT	CU	CV	CW	CX	CY	CZ	DA	DB
1	1180	1185	1190	1195	1200	1205	1210	1215	1220	1225	1230	1235	1240	1245	1250	1500
2	0.9898178	0.9899231	0.9899950	0.9900371	0.9900532	0.9900469	0.9900219	0.9899819	0.9899306	0.9898717	0.9898090	0.9897460	0.9896865	0.9896342	0.9895928	1.0000000

Spectral parameter maps are generated in worksheets 13 through 18 as follows:

Table A2.1 Maps generated within the worksheet

Sheet 13	Sheet 14	Sheet 15	Sheet 16	Sheet 17	Sheet 18
"Pyroxene" band center minimum	"Pyroxene" band center depth in per-cent	FWHM	"Olivine" band center minimum	"Olivine" band center depth in per-cent	OMAT (optical maturity)

In strict terms the Sheet 13 maps the principal trough center present, but this is almost invariably the pyroxene trough near 1000 nm. Sheet 16 maps the principal trough or

shoulder present beyond 1000 nm but under 1150 nm. For this reason pyroxene and olivine are placed in quotation marks in Table A2-1.

Customizing the polynomial fit function (for very advanced users with a knowledge of array functions and VBA programming):

Examples of routine maps automatically produced by the worksheet were shown earlier in this paper. Figures A3-1 through A3-4 shows some custom generated maps for Aristarchus produced by custom selecting a particular polynomial or spline fit to the continuum divided absorption trough. These require minor program code alterations to Macro 2 by the user, but are quite simple to achieve. Only a selected portion of the array for the polynomial fit is shown in cells beginning at AC3 in Sheet 10.

This array is expandable to provide data for up to a 20th order polynomial fit. In Figure A3-1 the generated absorption trough minimum band center map generated by the Excel program uses a 9th order polynomial fit.

Figure A3-2 shows the band depth map generated using a 3rd order (i.e. cubic) spline fit to the Clementine absorption trough data. Figure A3-3 is the FWHM map generated using a 5th order polynomial fit. Image A3-4 is a false color map of the crater created in the CAD program Rhino. The band depth is represented by height. The color overlay consists of the inverse of the trough minimum map in the red channel, the FWHM map in the green channel, and the trough minimum map in the blue channel.

Fig. A3-1

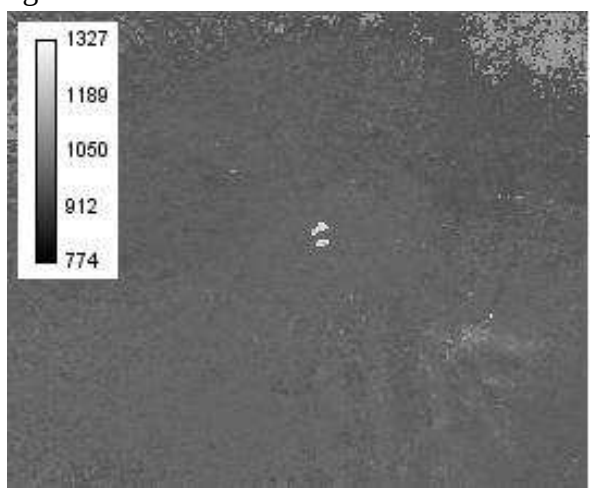

Fig. A3-2

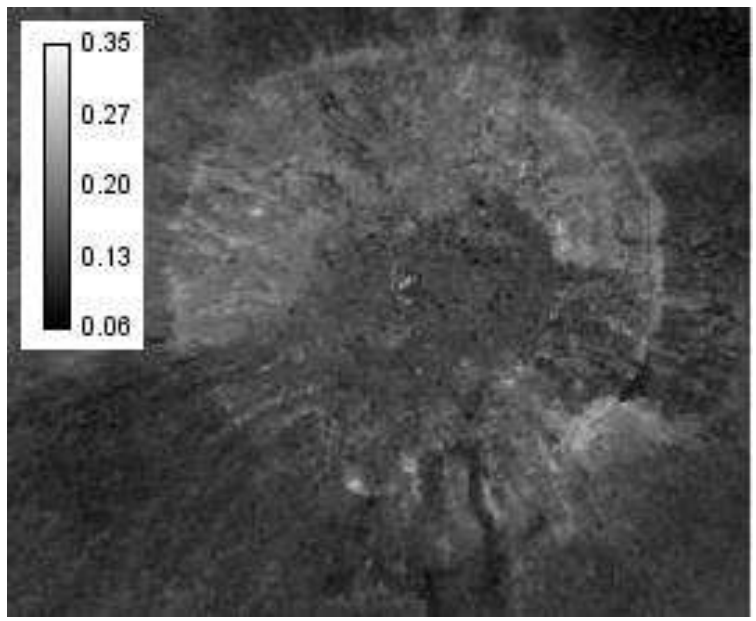

Fig. A3-3

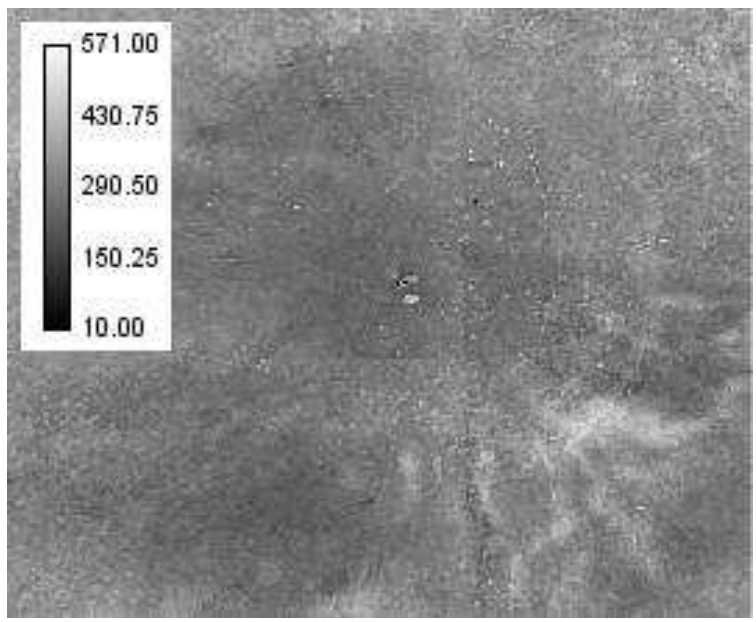

A3-4

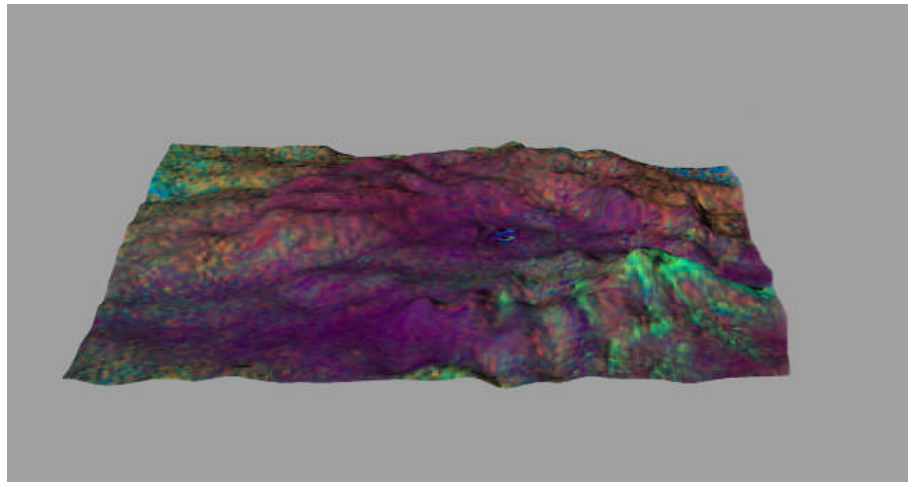

Appendix II: Exploration of Spectral parameter estimation described by LeMouelic (2000) and Lucey (1998)

The Clementine lunar probe imaged the lunar surface using five UV-visible spectral bands and six near infrared bands covering the wavelength range from 415 nm to 2780 nm. The five UV-visible bands have been available on the map-a-planet website maintained by the USGS for some years. Recently, however, the first four near infrared bands covering the range from 1100 nm to 2000 nm have been calibrated so that both datasets can be used seamlessly. Calibration for the last two near infrared bands (2600 nm and 2780 nm) is generally thought to be less reliable.

Examination of wavelength vs reflectance plots made from the 415 nm to 2000 nm calibrated images provides important information about the mineral composition of the moon. Information about the identity of iron bearing (mafic) minerals (pyroxenes and olivine) is contained in the parameters of an absorption trough near 1000 nm. Most lunar titanium is contained in the mineral ilmenite which absorbs near 415 nm. The 415 nm to 750 nm spectral ratio is proportional to the titanium content of lunar soils. Titanium concentration can be calculated using this ratio. The continuum slope, generally taken as the slope of a line connecting the reflectance value at 750 nm and 1500 nm, is steeper for more mature (i.e. weathered) lunar features and shallower for more recent, less weathered lunar features. This slope can be used to correct the depth of the mafic absorption trough near 1000 nm for the effects of weathering by micrometeorite bombardment and long term exposure to solar radiation. Weathering causes the absorption trough to become shallower and less deep. The trough characteristics can be restored by dividing reflectance values by the continuum slope. The total iron content of a lunar feature can be calculated from the concentration of mafic minerals and ilmenite ($FeTiO_3$), since the latter contains iron as well as titanium. The total iron content of a

lunar feature can be calculated from the slope corrected mafic trough depth and the titanium concentration.

The specific equations (listed below) relating reflectance to the parameters discussed above are discussed in great detail by Le Mouelic (2000) and by Lucey (1998). $R_{wavelength}$ refers to the pixel value of the Clementine image taken at that wavelength at the particular location being measured. Eq. 4 below requires that R_{750} be in absolute reflectance, which means that the pixel value must be multiplied by 0.000135.

(Eq. 1) Continuum Slope Determination

$$slope = (1/ R_{750}) * (R_{1500} - R_{750})/(1.5 - 0.75) \text{ abs. refl./micron}$$

This slope value is scaled to tangency at 0.75 microns

(Eq.2) Trough Depth Uncorrected for Continuum Slope

$$depth_1 = 1 - [(R_{950})/((2.2/3)R_{750} + (0.8/3)R_{1500}))]$$

(Eq. 3) Trough Depth Corrected for Continuum Slope

$$FeO_{mafic} = depth_1 + 0.286 * slope$$

The slope calculated in Eq. 1 was scaled to tangency at 0.75 microns

(Eq. 4) Titanium Oxide content in wt. %

$$TiO_2 = (\theta_{Ti}^2 * 20.79) - ((\theta_{Ti} * 22.928) + 5.909$$

(Eq. 4a) where: $\theta_{Ti} = \arctan [((R_{415}/R_{750}) - 0.45) / (R_{750} - 0.05)]$

and: R_{750} is in absolute reflectance (i.e. $R_{750} * 0.000135$)

(Eq. 5) Total Iron content in wt. %

$$\text{total FeO} = 45.6(depth_1 + 0.286 * slope) - 3.8 + 0.9\ TiO_2$$

Nine Clementine UV-visible and near infrared spectral bands covering the range from

415 nm to 2000 nm were downloaded in 16 bit TIFF format from the map-a-planet website maintained by the USGS (see http://www.mapaplanet.org/explorer/moon.html). A geographic area was selected and the color albedo (i.e. natural color) image was examined. The UV-visible bands 1 through 5 corresponding to 415 nm, 750 nm, 900 nm, 950 nm, and 1000 nm were requested individually in 16 bit tiff format. The database was then changed to the near infrared enhanced color database without changing the geographic location. Near infrared bands 1 through 4 corresponding to 1100 nm, 1250 nm, 1500 nm 2000 nm were then requested individually in 16 bit tiff format. The images were then converted to image txt format using the Import function in ImageJ. These txt images were processed using the Math and Image Calculator features under the Process Menu of ImageJ such that the mathematical requirements of each one of the six equations listed above was fulfilled by a single processed image constituting the spectral image map for the parameter defined by the equation. However, ImageJ could not be used to take the arc tangent as required by Eq. 4a and this was done by importing the txt file into EXCEL 2007 and applying the arc tangent function in radians on a spreadsheet containing the numerical matrix of the image. The processed image was then exported from EXCEL 2007 as a txt file and imported into ImageJ for use in constructing the spectral map corresponding to Eq. 4. At the conclusion of processing spectral map images corresponding to the continuum slope, the trough depth uncorrected for slope, the mafic trough depth corrected for continuum slope, the spectral angle θ_{Ti}, TiO_2 in wt. %, and Total Iron in wt. % were produced for Aristarchus and Alphonsus.

A4.1 Aristarchus Area

The spectral data have been analyzed and the continuum slope scaled to tangency at 750 nm, the trough depth uncorrected, the mafic trough depth corrected for continuum this slope, the spectral angle θ_{Ti}, TiO_2 in wt%, and Total Iron in wt% were produced in order to assess their maturity and mineralogical composition. Figures A4.1a through A4.1h were created using Eq. 1 through Eq. 5.

In the spectral map of continuum slope (Figure A4.1a) dark areas correspond to younger, less weathered, regions (e.g part of central peak and east wall). Note that for the most part the central peak is saturated so that it is not possible to carry out a specific analysis. The process of surface maturation causes a reddening of the surface spectra (increase of a positive slope) and a decrease of the spectral contrast of the absorption bands.

The spectral map of trough depth corrected for continuum slope (Fig A4.1c) obtained from Fig A4.1b after correction for continuum slope scaled to tangency at 750 nm (Fig A4.1a) displays the FeO mafic content. The SE wall regions and part of the central peak shows lowest FeO mafic content in the Aristarchus crater.

A4.1a Spectral map of continuum slope

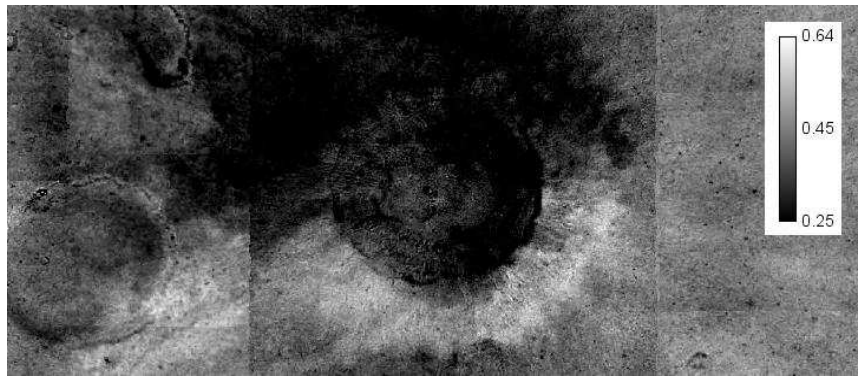

Fig. A4.1b: Spectral map of trough depth uncorrected for continuum slope

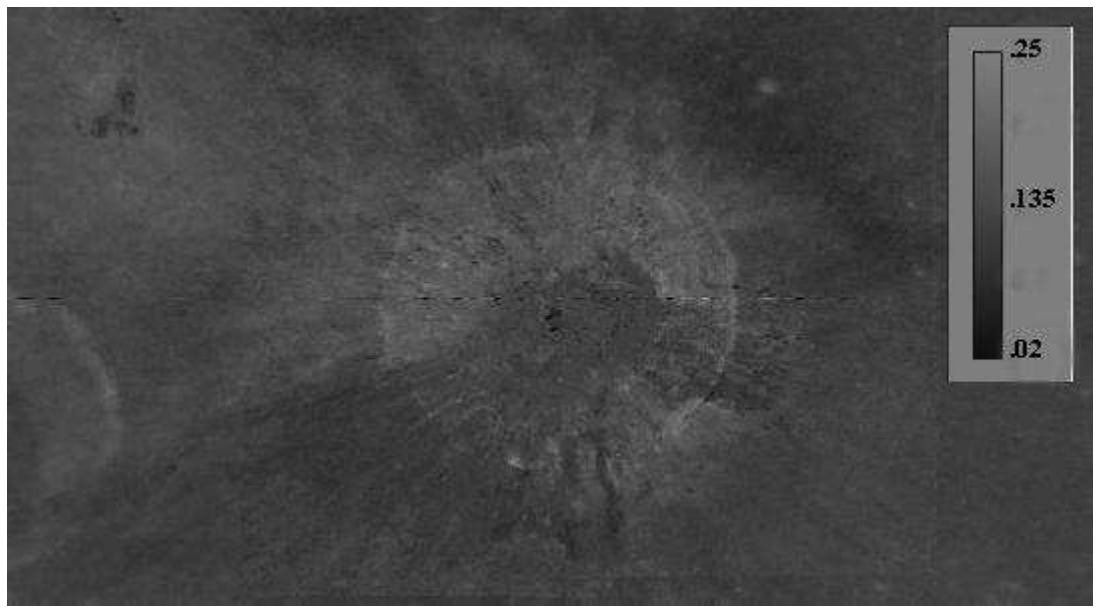

Fig. A4.1c: Spectral map of trough depth corrected for continuum slope (FeO mafic

content wt%)

Ilmenite is a Titanium oxide in varying abundance in the lunar maria and the maps of Fig. A4.1e, produced by the inferred spectral angle θ_{Ti} (Fig 1d) displays the inferred TiO_2 content in wt%. As expected from previous studies by Le Mouelic et al (2000) the map shows a very low ilmenite content.

Fig. A4.1d: Map of spectral angle θ_{Ti}

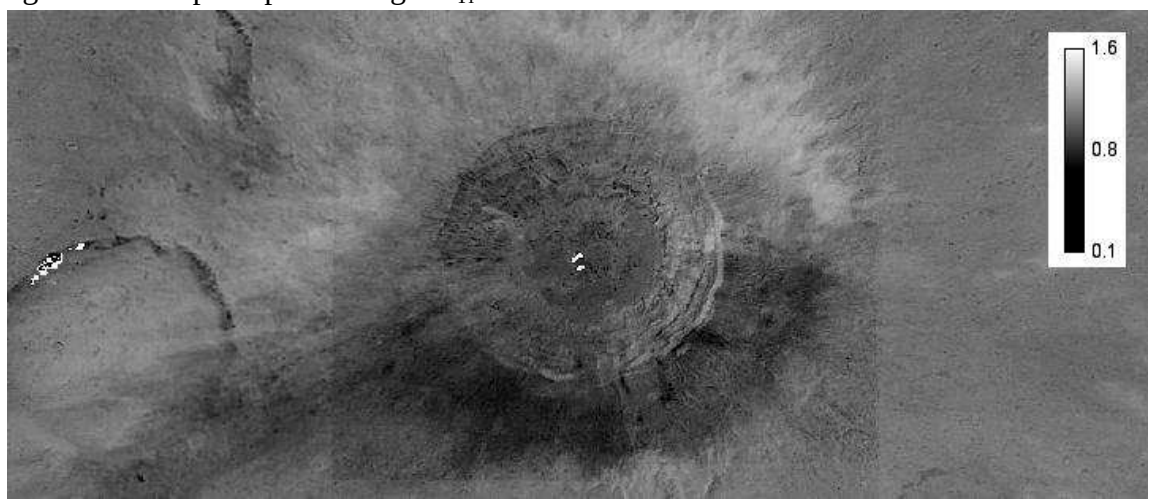

Fig. A4.1e: Spectral map of TiO_2 in wt%

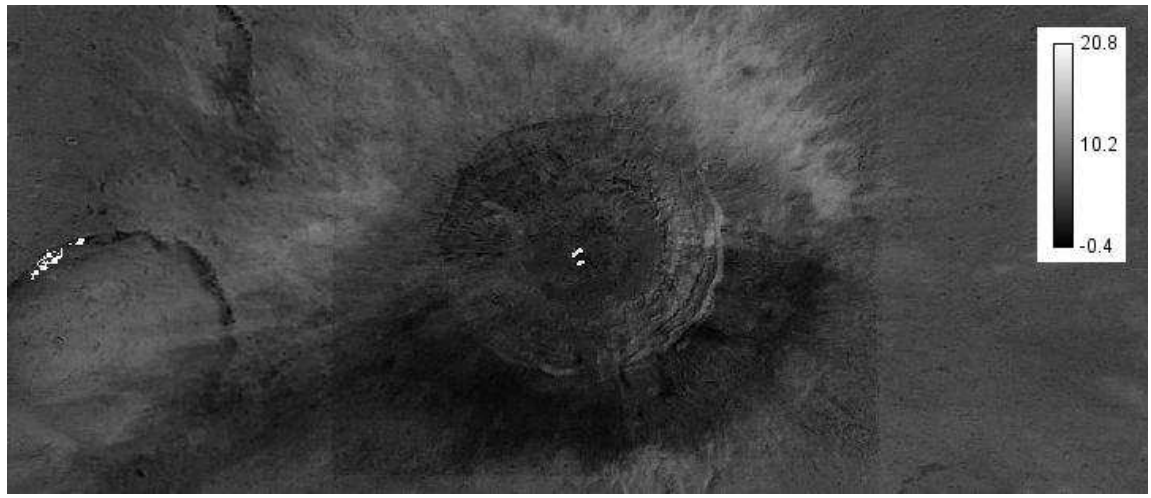

The use of the equations (1-5), reported in the introduction, allow us to obtain the total Iron in wt% (Fig 1f and the corresponding color gradient map shown in Fig. A4.1g), discriminating highland type material (low-intermediate FeO content) and mafic material (intermediate to high FeO content). The lowest FeO content is found in the unsaturated portion of the central peak (4%) while the highest FeO content is detectable in the dark mantle deposit covering the north eastern part of the ejecta material.

Fig. A4.1f: Spectral map of Total Iron in wt%

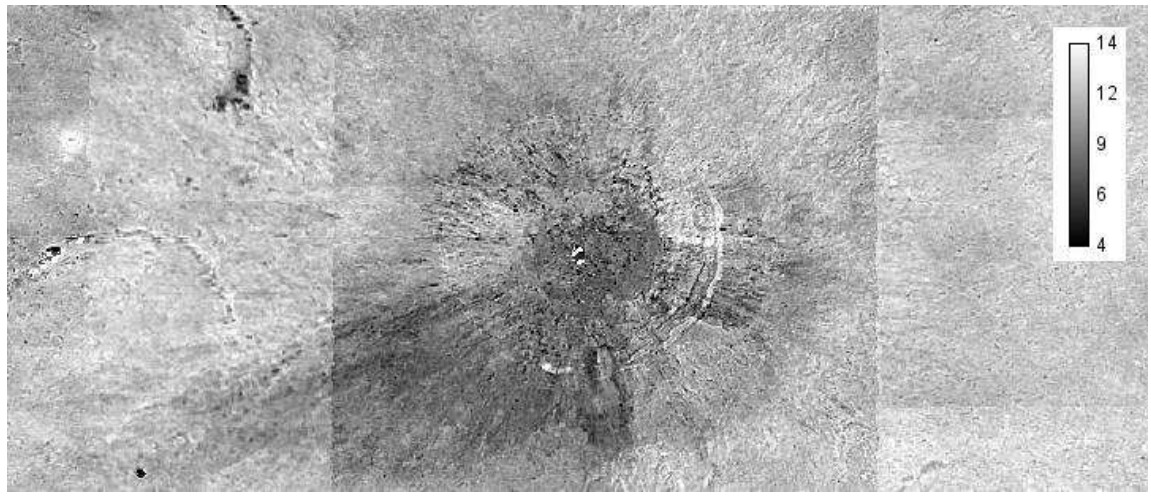

Figure A4.1g: color gradient map of Total Iron in wt %

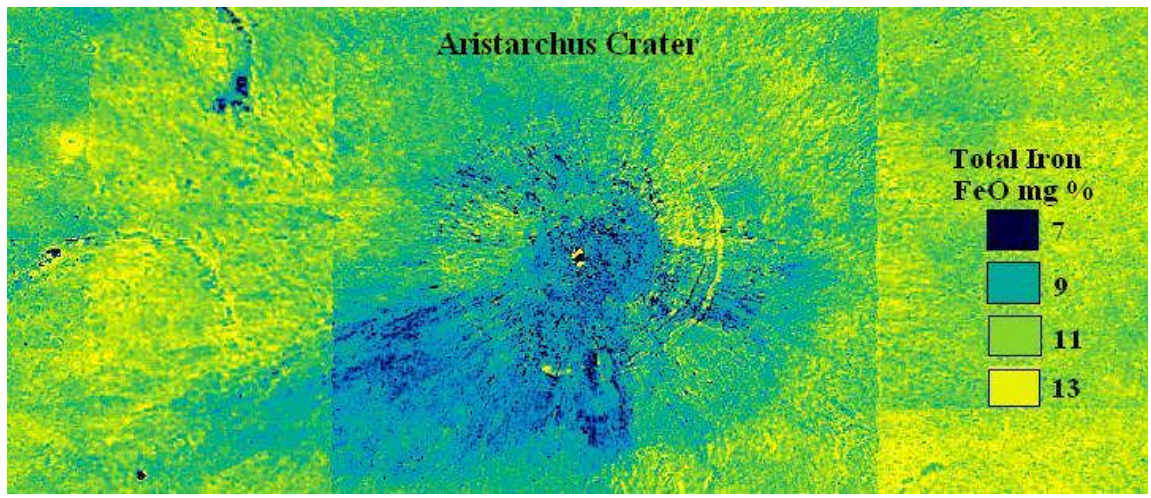

The presence of olivine is inferred from the color ratio mosaic image where the ratio 1250/1500 is assigned to the red channel, the ratio 1100/1500 to the green channel and the ratio 2000/1500 to the blue channel. In the composite image the olivine deposit is identified for the deep blue hue, while pyroxenes show bright yellow hue (Fig. 4.1h).

Figure A4.1h: color composite image, the olivine deposits identified for deep blue color

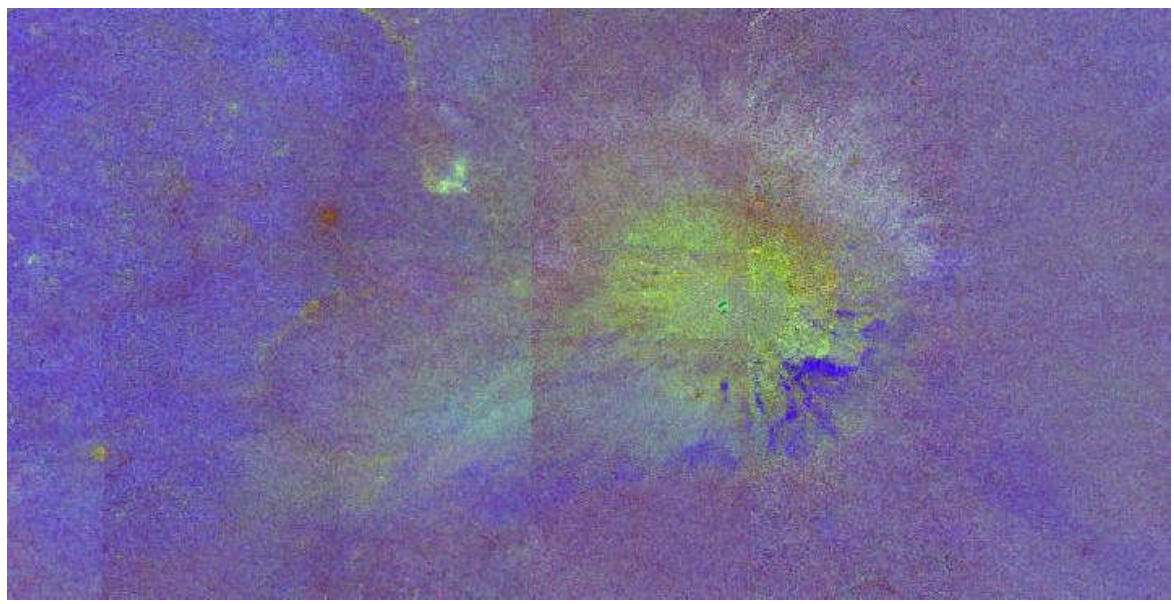

This color ratio image discriminates between pyroxenes and olivine areas. In Fig. A4.1i the band center for clinopyroxene, olivine and glass material is shown as bright white regions, while the orthopyroxene (including noritic material) is dark. The Aristarchus east floor displays band center in the range of 960 to 990 nm typical of high Ca pyroxene (clinopyroxene).
Two olivine deposits (cfr. Fig A4.1h and A4.1i) are identified in the southeastern wall and south wall at 4 and 6 o'clock respectively.

The absorption trough minimum values can be read from the band center estimation map shown in Fig. A4.1 i below by the relation:
trough minimum [nm] = 925 + (200/255)*greyvalue.
In Fig. A4.1j the absorption trough depth values can be read from the calibration bar. In Fig A4.1 k of the FWHM (full width at half maximum) map for Aristarchus, the FWHM values can be read by the relation:
FWHM value [nm] = 150 + (300/255)*greyvalue.

Figure A4.1i: Absorption Trough Minima Map (i.e. Band Center Estimation Map) created in Octave

Fig. A4.1 j Absorption trough depth map created in Octave

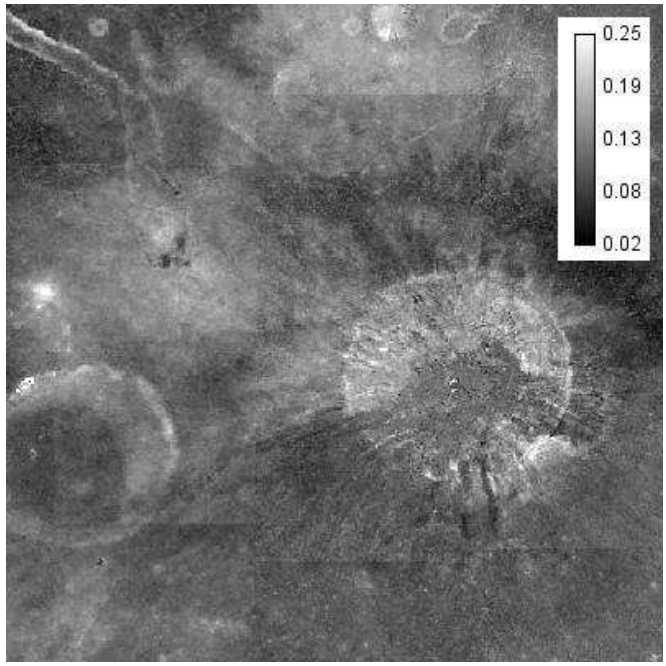

Fig. A4.1k FWHM map

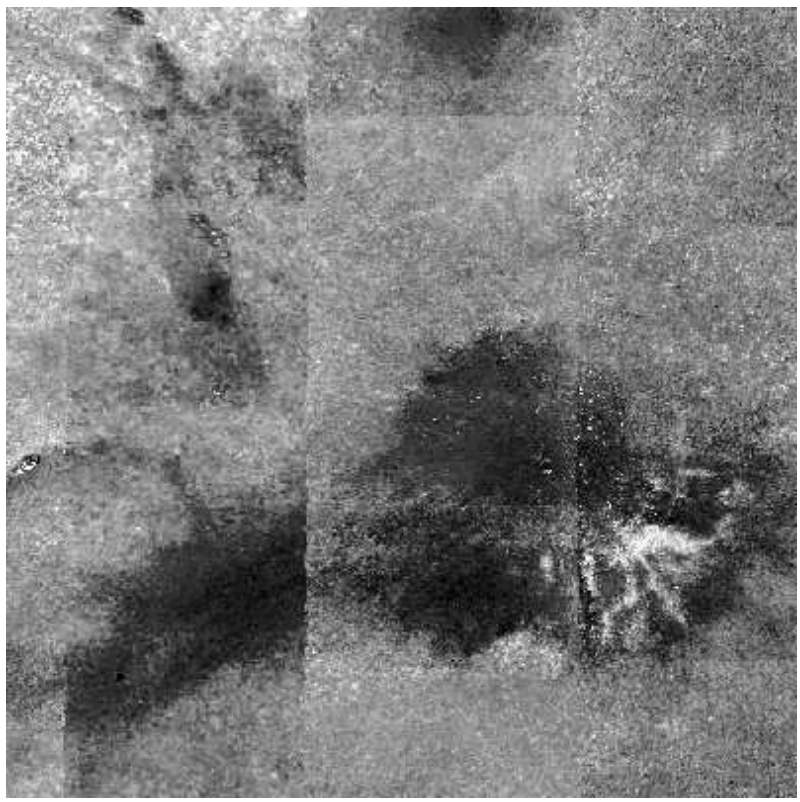

The band center of the large olivine rich deposit, located on the SE wall, was measured for a box area of 5X5 pixels. The absorption band was determined at 1047+/- 26 nm.
The second, smaller, deposit is recognized to the south, with an absorption band, for a box of 3x3 pixel, centered at 1034 nm +/- 16 nm. The absorption band, for two mentioned deposits, have a depth (uncorrected for maturity effect) of 0.185 +/- 0.029 and 0.119 +/0.013 respectively.
The corresponding FeO mafic, which is the trough depth corrected for continuum slope, was computed as 0.247 +/- 0.024 wt % and 0.322 +/- 0.030 wt%.

The total Iron computed from the equation (1), and the map 1f, yield a content of 9.528 +/ 1.512 FeO wt% and of 7.984 +/ 0.593 FeO wt% respectively for two olivine rich units. The inferred spectral results, if compared with the extracted spectra for a range of terrestrial olivine samples, suggest the presence of a low ferroan, magnesian olivine. A positive match was found with terrestrial sample Fo 91, for which the 1-µm band position is centered at 1043 nm with a compositional analysis of FeO 7.93 wt %, MgO 50.70 wt% , SiO_2 40.06 wt% , including very low amount of TiO_2 of 0.14 wt%.

We have also assessed the shape of the five band spectra for two boxed areas corresponding to the olivine rich unit (located to the southeastern wall) and to the central west floor of Aristarchus (see Fig A4.1n, Fig. A4.1o and A4.1p).
The spectrum of examined olivine rich deposit (Fig. A4.1j) indicates a troctolite (T) composition when compared with the predictive diagram by Tompkins and Pieters (1999).

Fig. A4.1 l Key to Aristarchus Feature Locations for Table A4.1-1

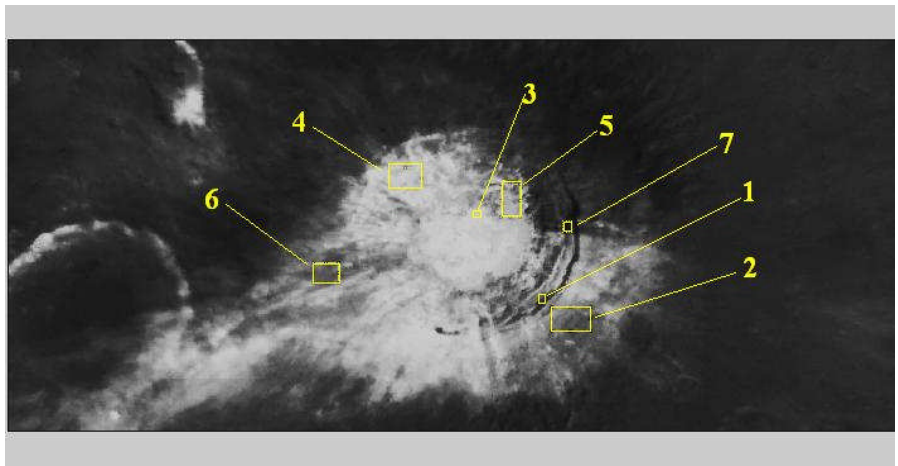

Table A4.1-1

Crater Feature (letter corresponds to labelled image)	Total Iron in wt% (note: method not valid for pyroplastic deposit assessment)	Band Center Estimate in microns	Relative Absorption Depth %	% Depth Uncorrected for Slope	Continuum Slope scaled to tangency at 750 nm
Area #1	11.2	.999	10.03	14.5	.242
Area #2	10.1	1.04	10.63	15.1	.460
Area #3	10.2	.998	5.63	10.1	.300
Area #4	9.4	.987	8.83	13.3	.300
Area #5	9.6	.973	11.33	15.8	.197
Area #6	9.9	.984	10.73	15.2	.269
Area #7	14.1	.974	10.53	15.0	.222
Central Peak	----	------	0	4.5	.091

Fig. A4.1 m

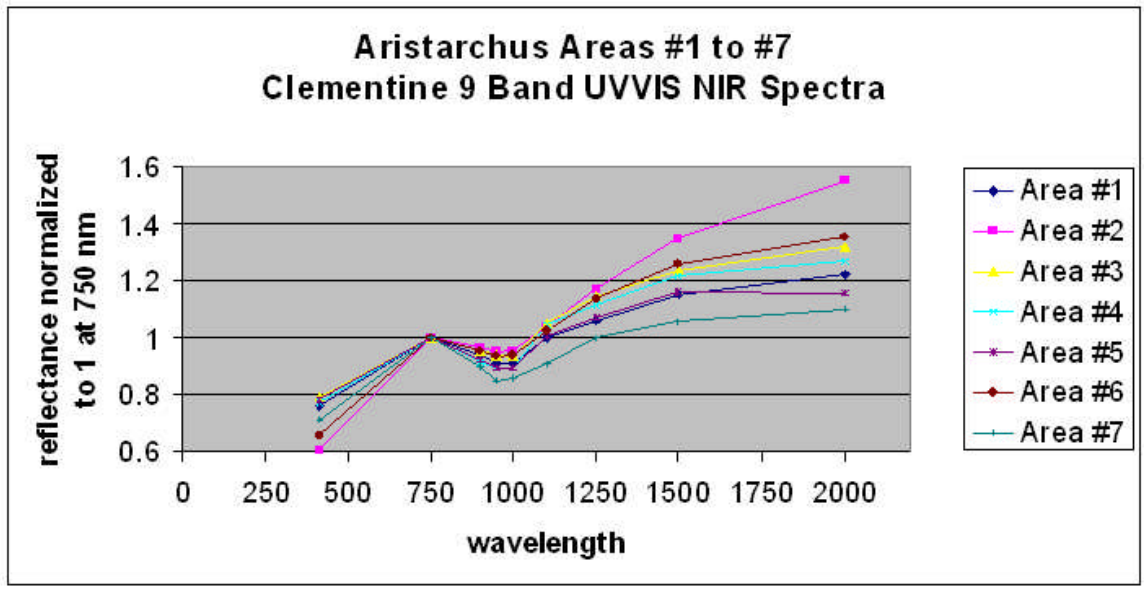

Fig. A4.1 n

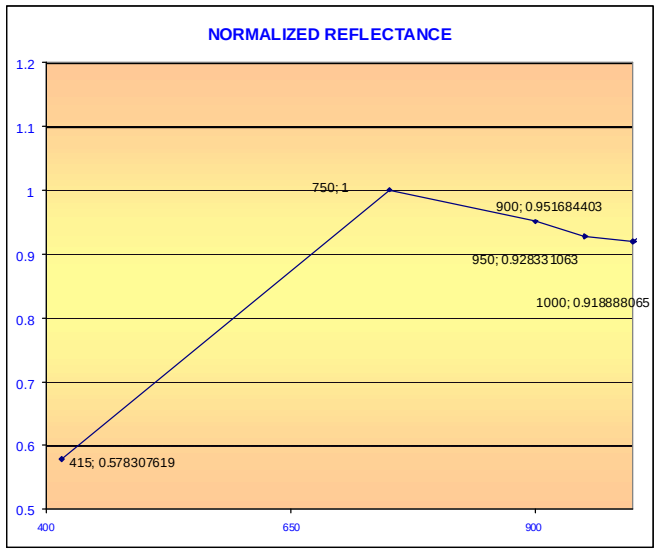

The spectrum of examined olivine rich deposit indicates a troctolite composition.
The spectrum of examined area located on the west floor of the crater (Fig. A4.1l) indicates a plausible anorthositic gabbro (AG) composition when compared with the predictive diagram by Thompkins and Pieters (1999). The Clementine 5 band UVVIS spectra of Area #2 is indicative of troctolite (Fig. A4.1 m) and the 9 band UVVIS-NIR spectra are also consistent with this interpretation (Fig. A4.1 k).

Fig. A4.1o

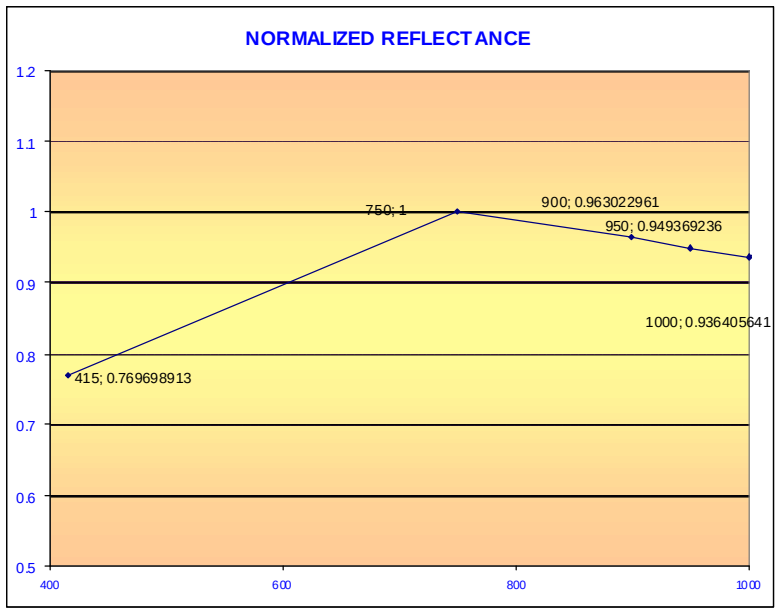

Figure A4.1p.

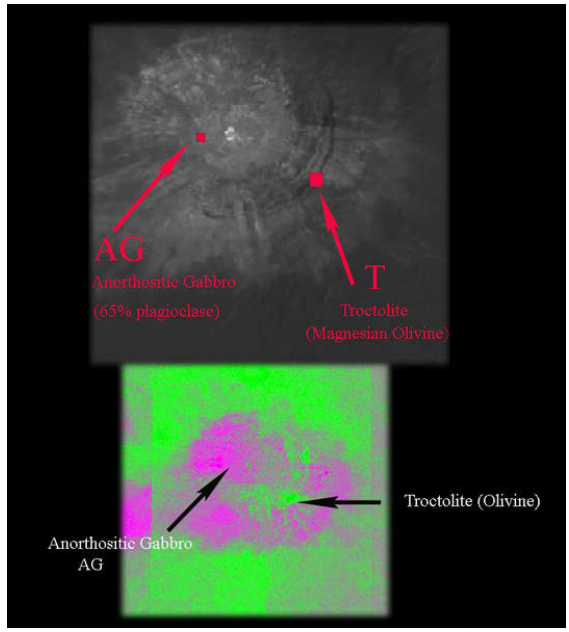

Accordingly, with the Fig. A4.1q, we have derived a false color mineral composition map, where the areas of weak mafic concentration, that are primarily feldspathic, appear pastel pink. The presence of a noritic component (intense red color) is excluded in Aristarchus. In Fig. A4.1r, created using the CAD program Rhino, the band depth is represented topographically as the height of lunar features while the false color overlay has the inverted band center map in the red channel, the FWHM map in the green channel, and the non-inverted band center map in the blue channel.

A4.1q Mineral mapping of Aristarchus Area

Fig. A4.1q

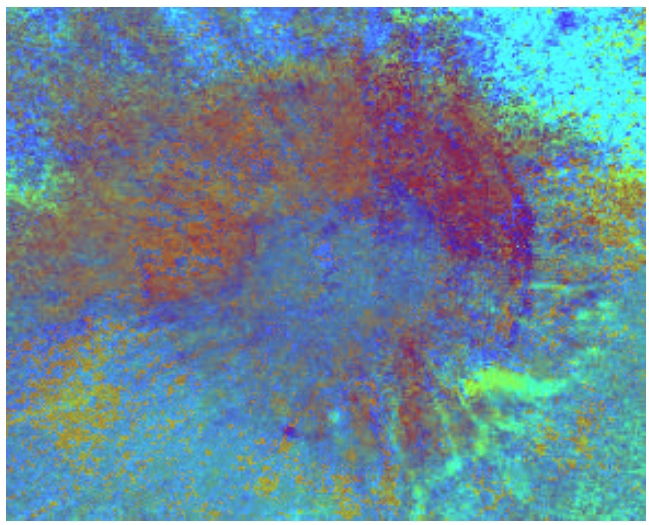

Fig A4.1r

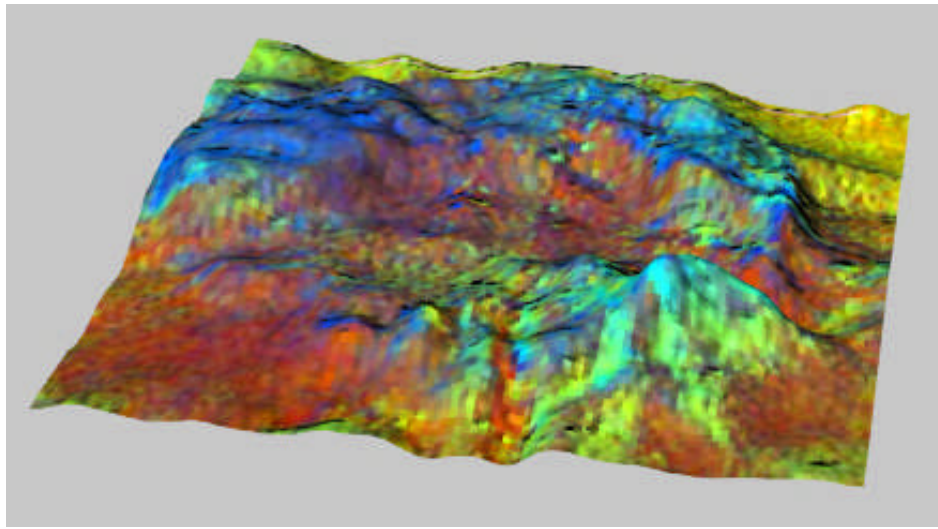

Inverse images were created using Photoshop CS2 using the Image>>Adjustment>>Inverse menus.

Mapping reveals several compositional units exposed within the crater, all being either weakly mafic or gabbroic (Figure A4.1q). The generated map indicates that the western floor and the western wall exposes mainly plagioclase likely with a small clinopyroxene component (rusty orange). The same unit is located to the southwest around the two localized olivine deposits (in bright green color). The shape of the extracted spectra, compared with the model described by Tompkins and Pieters (1999), suggests an anorthositic gabbro unit (AG), with a content of plagioclase of about 65%.
The rest of the crater appears to expose gabbroic units which appear blue in the color map.

The southeastern wall and a small portion of the south wall reveal a more olivine-rich unit, which is characterized for a troctolite composition. The inferred data in this work reveal the presence of a magnesian olivine (MgO about 50%) with lower FeO content in the forsterite (Mg_2SiO_4)-fayalite (Fe_2SiO_4) olivine solid solution series. The large bright area above and to the right of the crater is artifactual.

A4.2 Alphonsus

With the same procedure described for Aristarchus we have analyzed the continuum slope, the trough depth uncorrected for slope, the mafic trough depth corrected for continuum slope, the spectral angle θ_{Ti}, TiO_2 in wt. %, and Total Iron in wt. % . Results for a number of regional features are presented in Table A4.2 –1.

Figs. A4.2a and A4.2b show the spectral map of continuum slope scaled to tangency at 750 nm and the trough depth uncorrected for continuum slope. Fig. A4.2c shows the spectral map of the trough depth corrected for continuum slope scaled to tangency at 750 nm. The DHC's in Alphonsus have an unrealistically low total iron value as shown in Fig. A4.2g and A4.2h. In Lucey (1998) it is stated that the iron mapping is not reliable for pyroclastic deposits and that their measurement with the method should be avoided. Figures A4.1i and A4.2j are maps of the absorption trough minima and absorption band depth respectively. The values can be read from the greyscale as follows:
absorption trough minimum [nm] = 900 + (400/255)*greyvalue and absorption trough band depth can be read from the calibration bar.

The FWHM width in nm can be read from Fig. A4.2k by the relation:
FWHM = 125 + (225/255) * greyvalue.

Figure A4.2a: Spectral map of continuum slope scaled to tangency at 750 nm

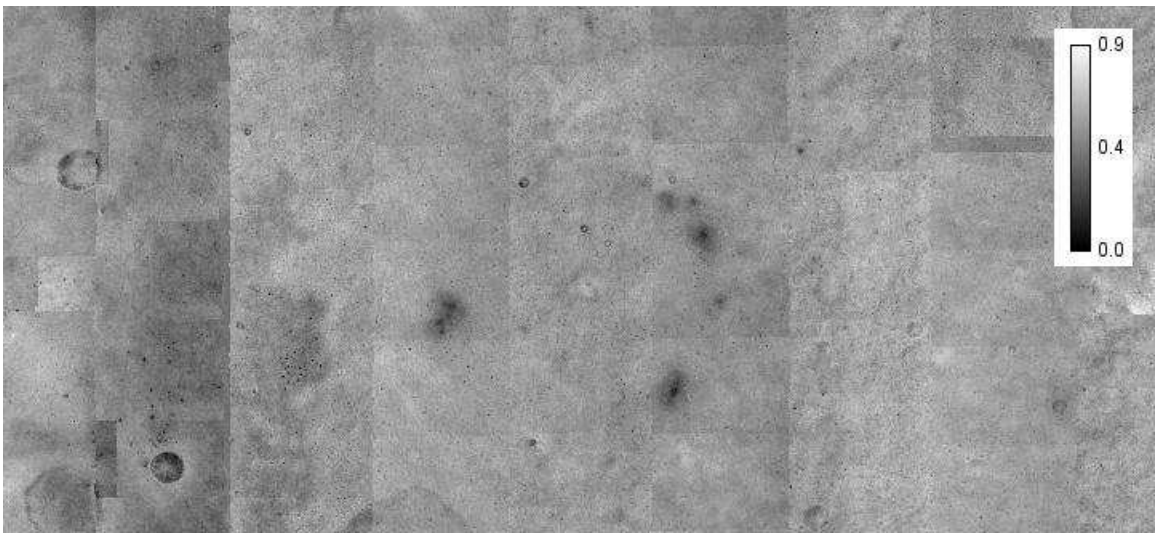

Figure A4.2b: Spectral map of trough depth uncorrected for continuum slope

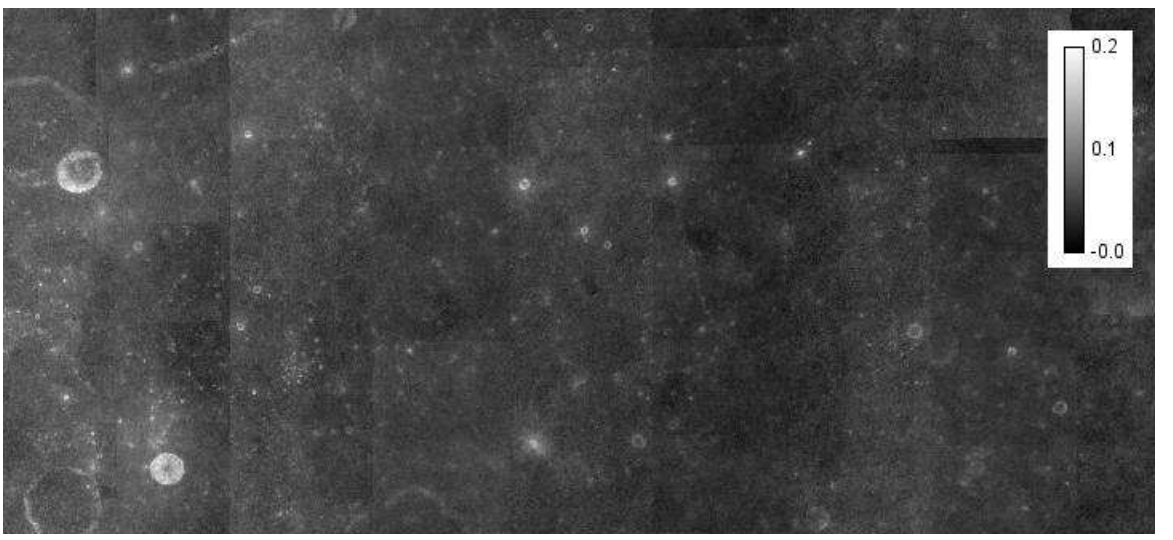

Figure A4.2c: Spectral map of mafic trough depth corrected for continuum slope scaled to tangency at 750 nm

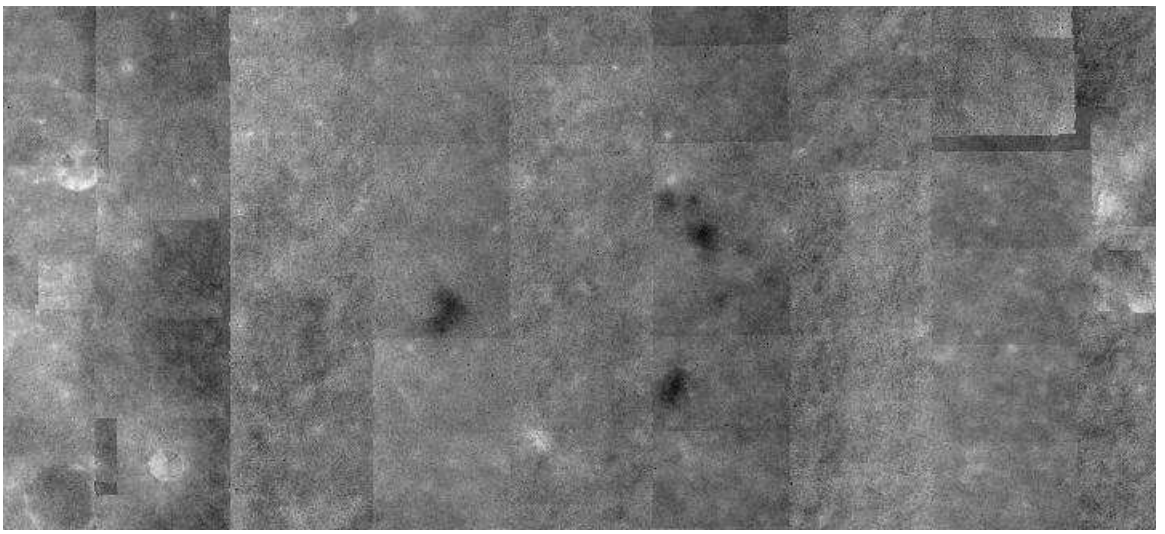

Figure A4.2d: Map of spectral angle θ_{Ti}

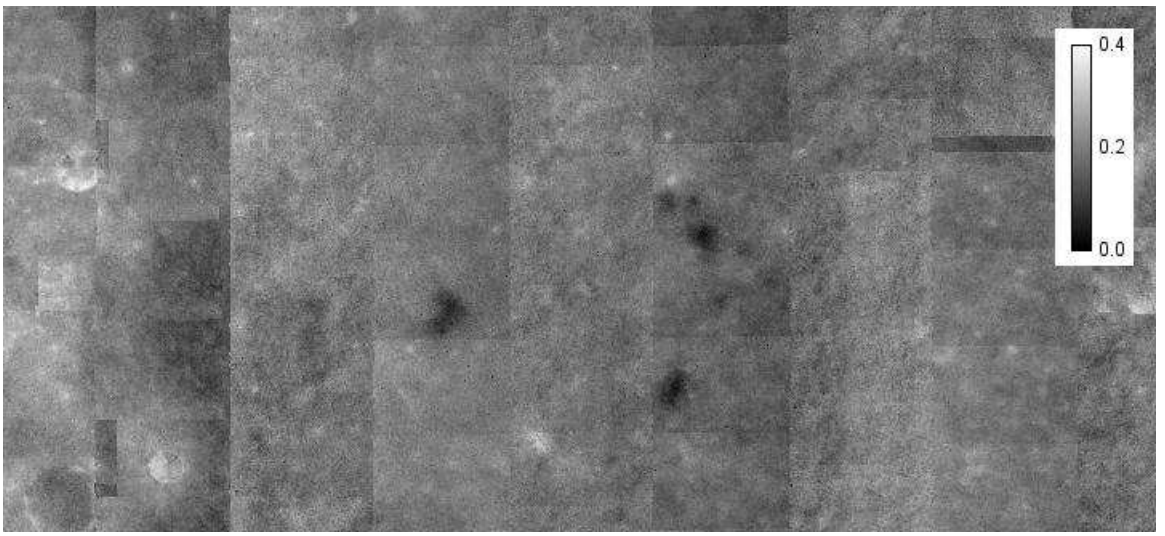

Figure A4.2e: Spectral map of TiO_2 in wt %

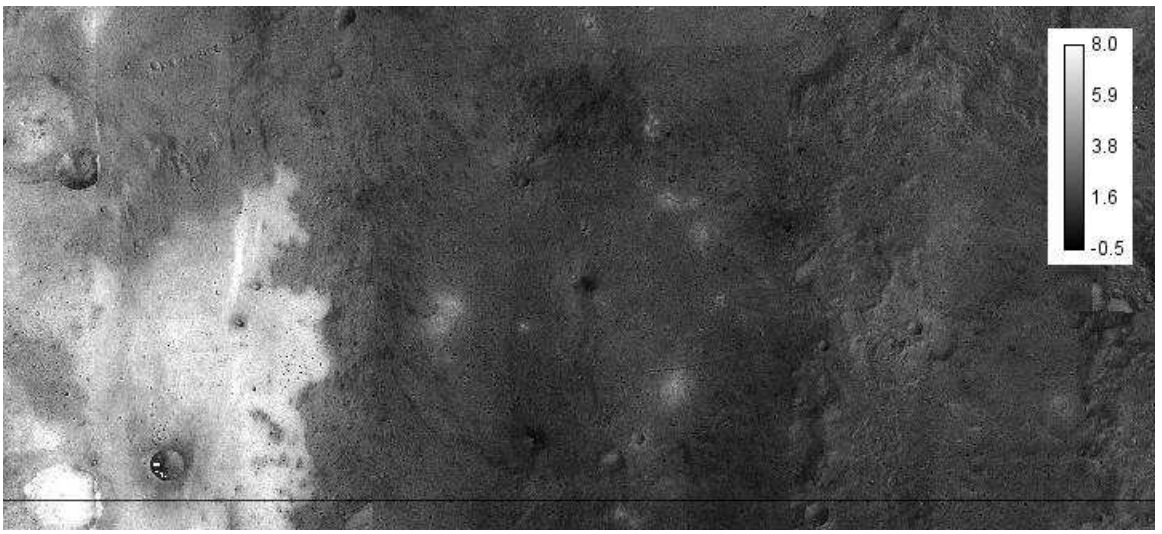

Figure A4.2f: Color map of TiO_2 in wt %

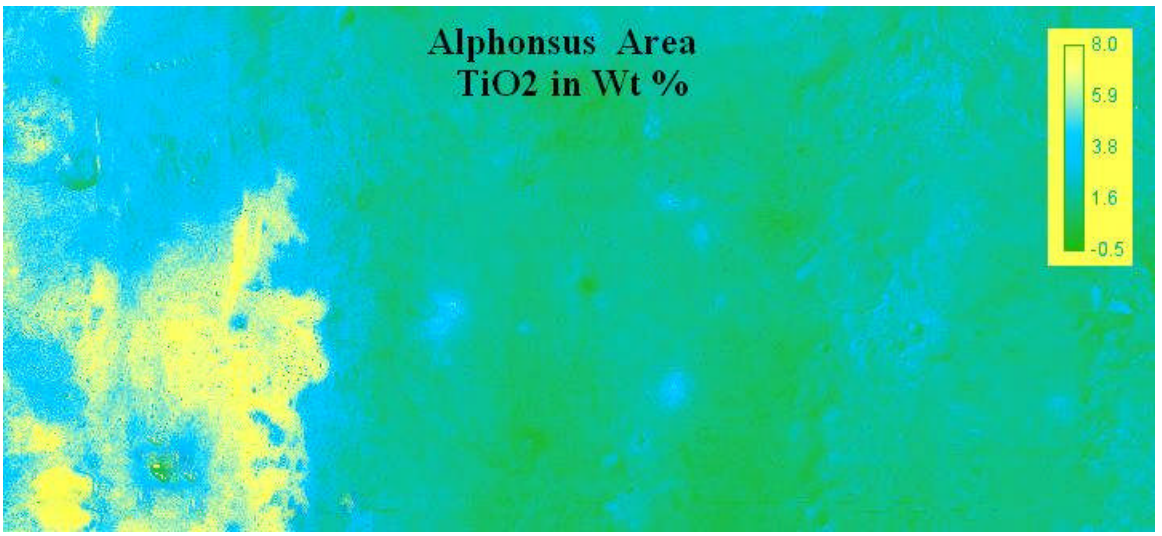

Figure A4.2g: Spectral map of Total Iron in wt %

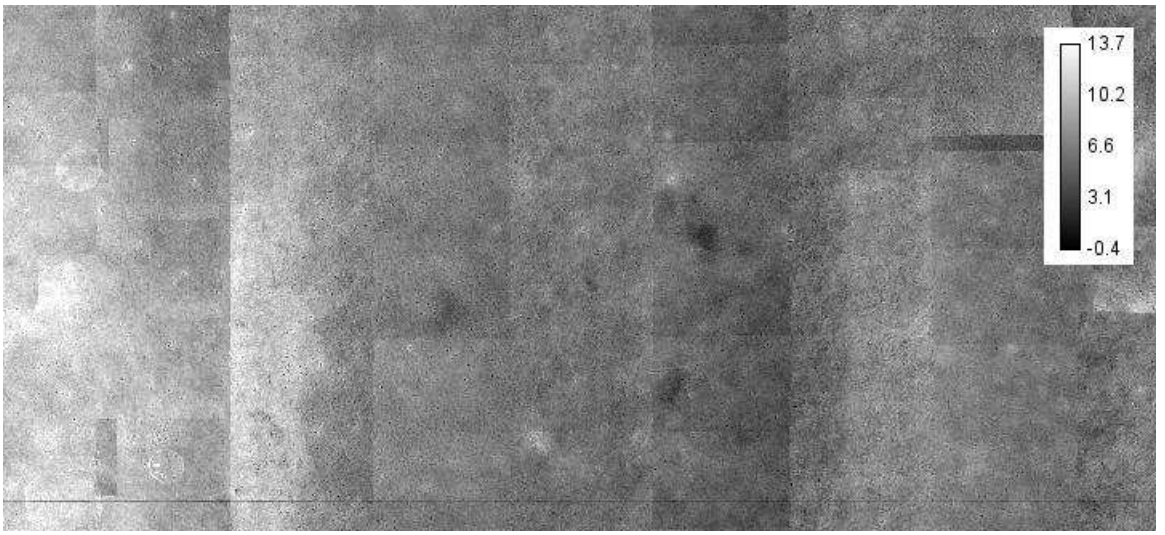

Figure A4.2h: Color gradient map of Total Iron in wt %

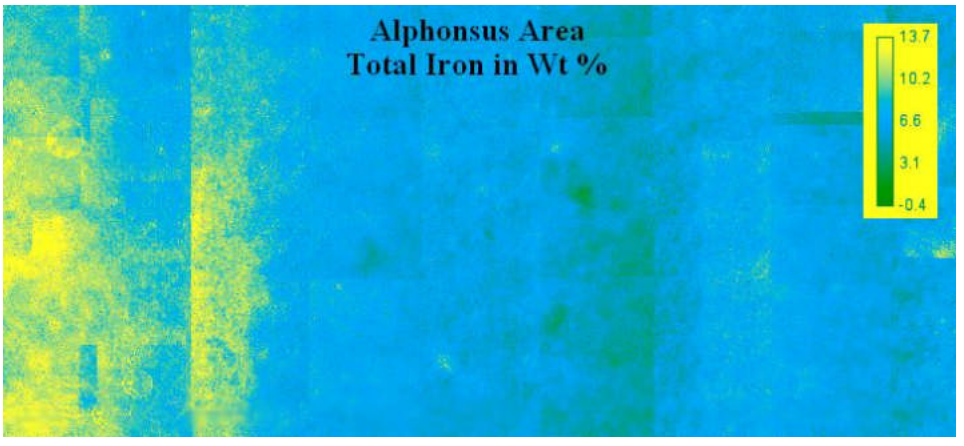

Figure A4.2i: Alphonsus absorption trough minimum map:

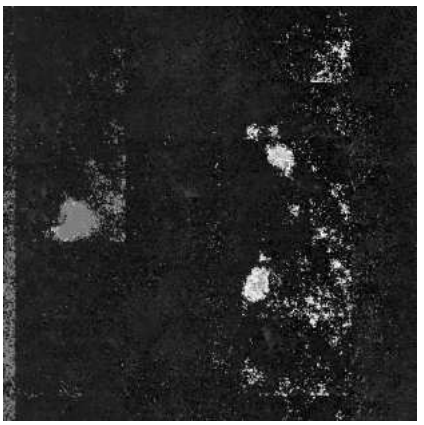

A4.2 j: Alphonsus absorption trough depth map

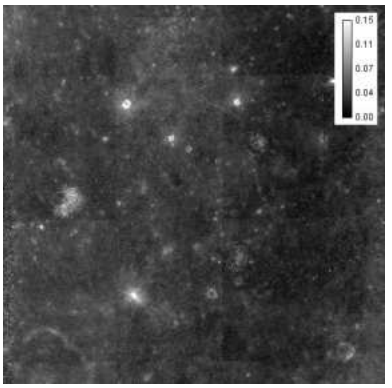

Fig. A4.2. k FWHM map

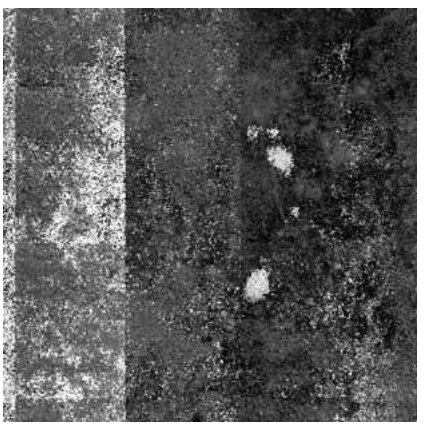

Fig. A4.2 l Excel Maps

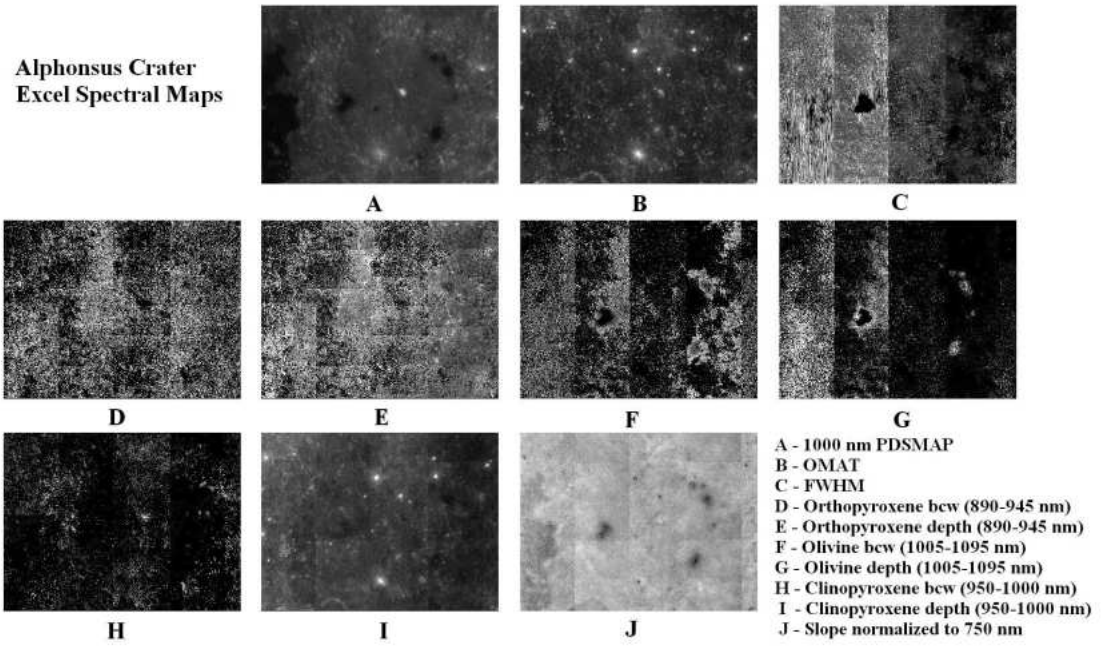

Fig. A4.2 m Geographic Key to Table A4.2 - 1

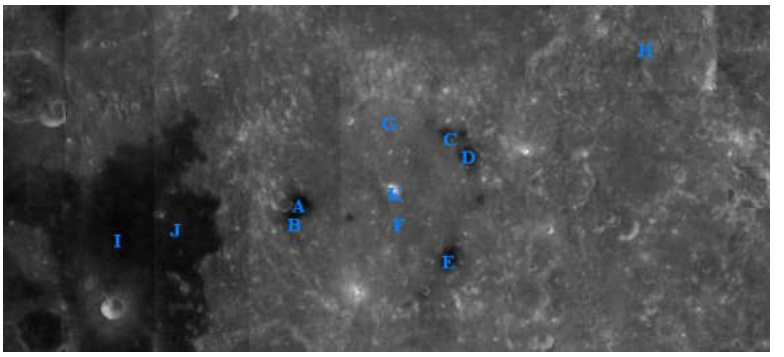

Crater Feature (letter corresponds to labelled image)	Total Iron in wt% (note: method not valid for pyro-plastic deposit assessment)	Band Center Estimate in microns	Relative Absorption Depth %	% Depth Uncorrected for Slope (Eq. 2)	Continuum Slope scaled to tangency at 750 nm
Floor of crater (F)	5.6	0.925	3.5	2.8	.503
Floor of crater (G)	6.4	0.935	1.9	4.1	.519
DHC West #1 (A)	------	1.0 to 1.015	8.5	2.2	.306
DHC West #2 (B)	------	1.010 to 1.040	8.0	1.8	.317
DHC East #1 (C)	------	1.013 to 1.033	6.9	0.7	.320
DHC East #2 (D)	------	1.019 to 1.040	11.0	0.9	.256
DHC East #3 (E)	------	1.026 to 1.085	10.8	1.0	.160
NW Highlands (H)	6.0	0.895 to 0.945	5.9	3.8	.543
Central Peak (K)	7.0	0.890 to 0.925	0	1.5	.571
Mare Nubium #1 (I)	9.6	0.958	3.0	5.4	.386
Mare Nubium #2 (J)	10.3	0.960	2.0	3.8	.478

Table A4.2 - 1

Figure A4.2n Five Band UVVIS Spectra of Regional Features

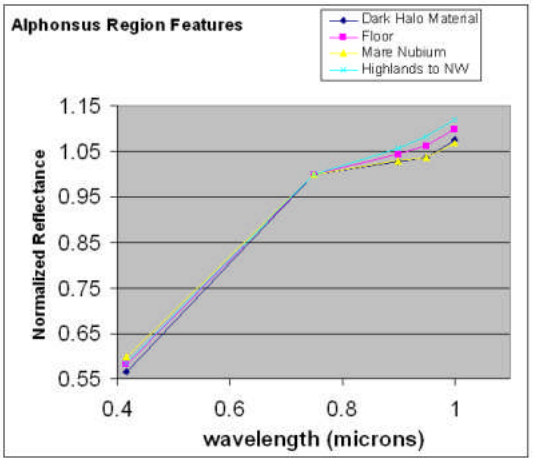

Fig. A4.2o Alphonsus Dark Halo Material 9 Band UVVIS-NIR Spectra

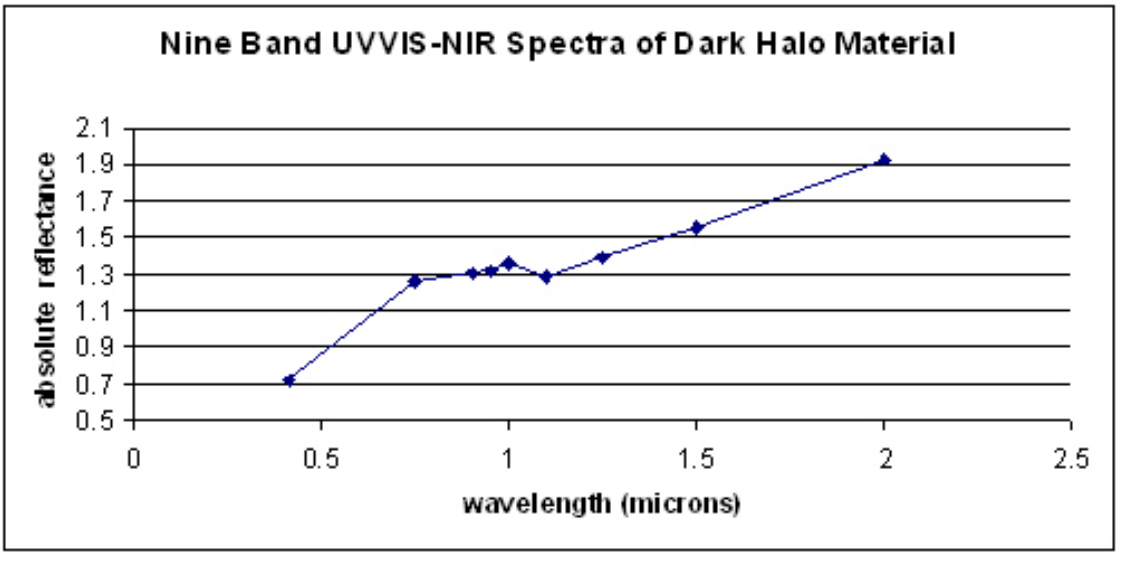

Figure A4.2 p: False Color Mineral Composition Map

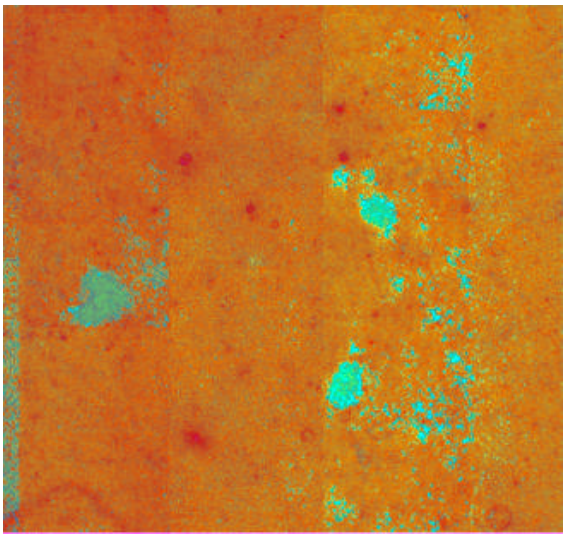

The false color map in Fig. 4.2 p below has height controlled by the band depth map while the false color overlay has the inverse of the band center map in the red channel, the FWHM map in the green channel, and the band center map in the blue channel.

Fig. A4.2 q: False Color Topographic Map

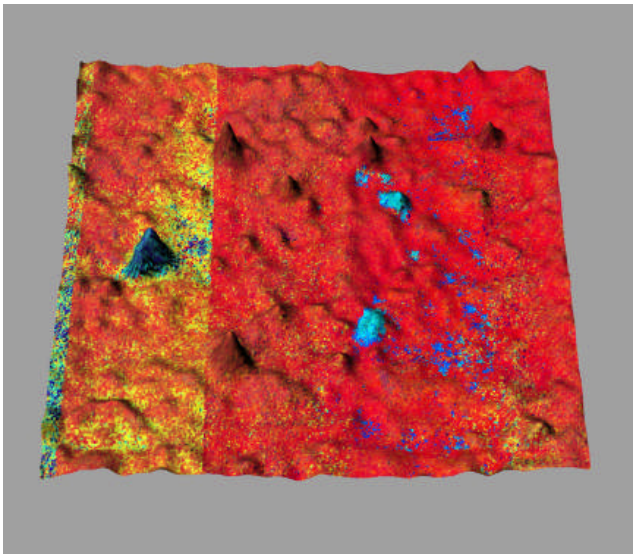

A4.3 Bullialdus

Using the same procedure described we have analyzed the continuum slope scaled to tangency at 750 nm, the trough depth uncorrected for this slope, the mafic trough depth corrected for this continuum slope, the spectral angle θ_{Ti}, TiO_2 in wt. %, and Total Iron in wt. % . We also made a θ_{bc} map and a band center estimation maps of Bullialdus as well as false color images using the latter and the [2000/1500 nm] ratio image.
The central peaks are very noritic with deep mafic bands. The crater walls are gabbroic but mixed with noritic material in some areas. Crater ejecta is gabbroic.

The absorption trough minimum map in Fig. 4.3i can be read by the relation:
trough minimum = 900 + greyscale value * 150/255.

The absorption trough depth map in Fig. 4.3j can be read from the calibration bar. The FWHM width in nm can be read in Fig. 4.3k from the relation:
FWHM = 180 + (220/255) * greyscale value.

Fig. A4.3 a Map of Continuum Slope scaled to tangency at 750 nm

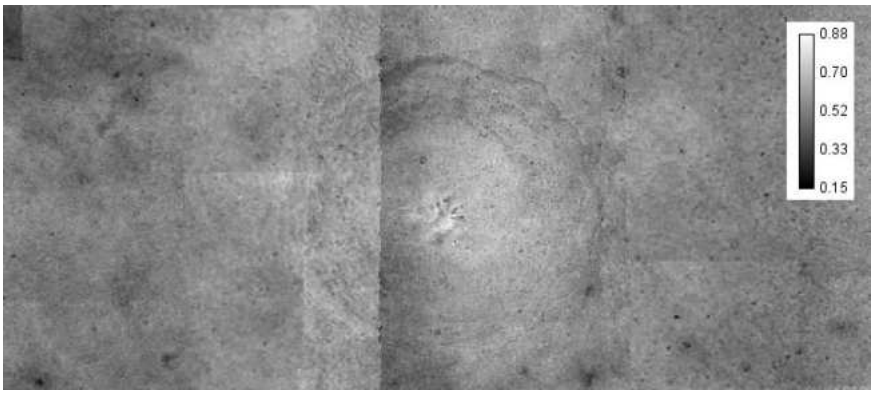

Fig. A4.3 b Trough Depth Uncorrected for Continuum Slope

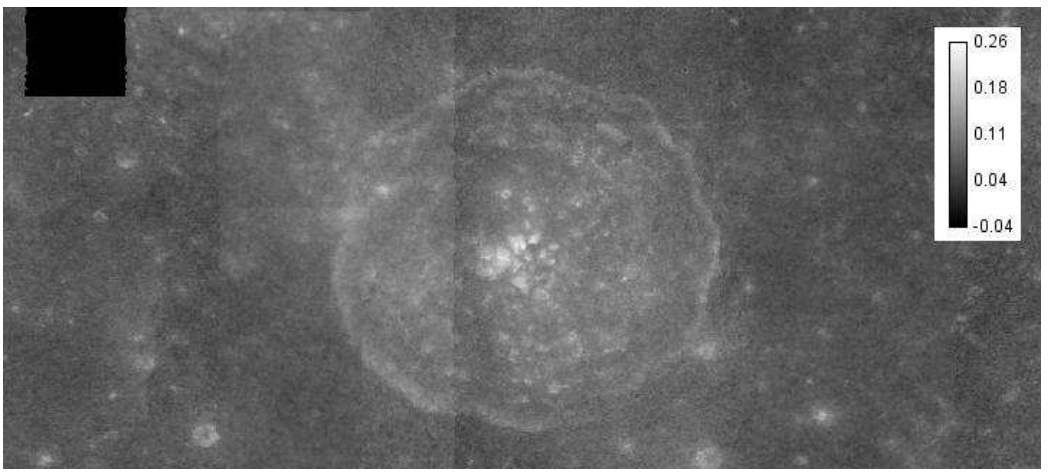

Fig. A4.3 c Mafic Depth Corrected for Continuum Slope scaled to tangency at 750 nm

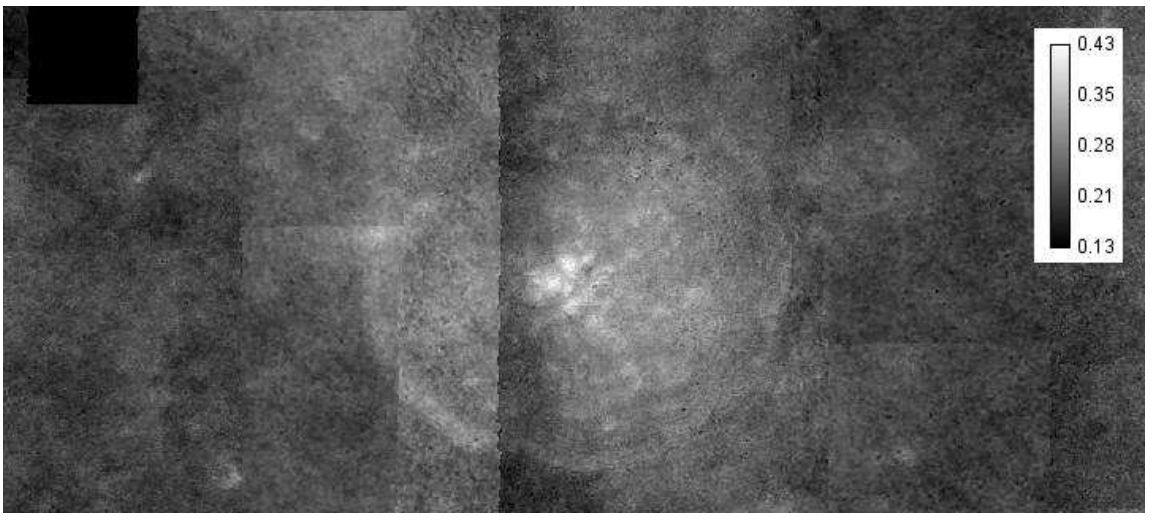

Fig. A4.3 d Theta Ti

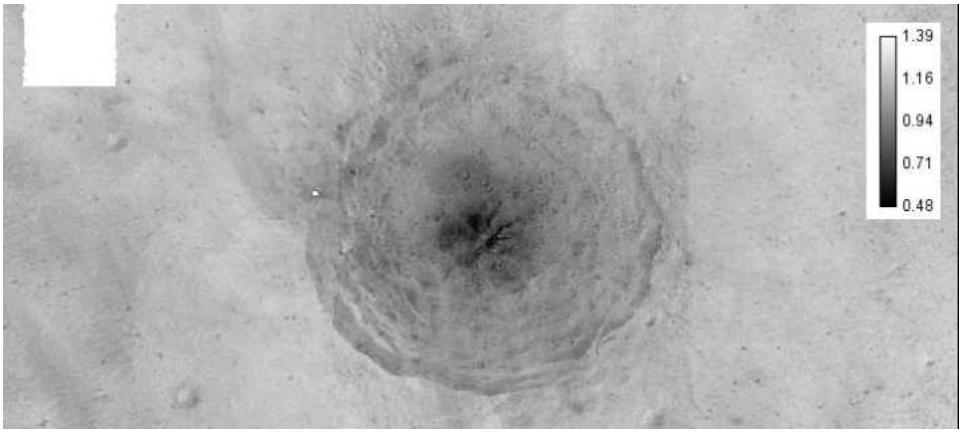

Fig. A4.3 e Titanium Map Color Gradient

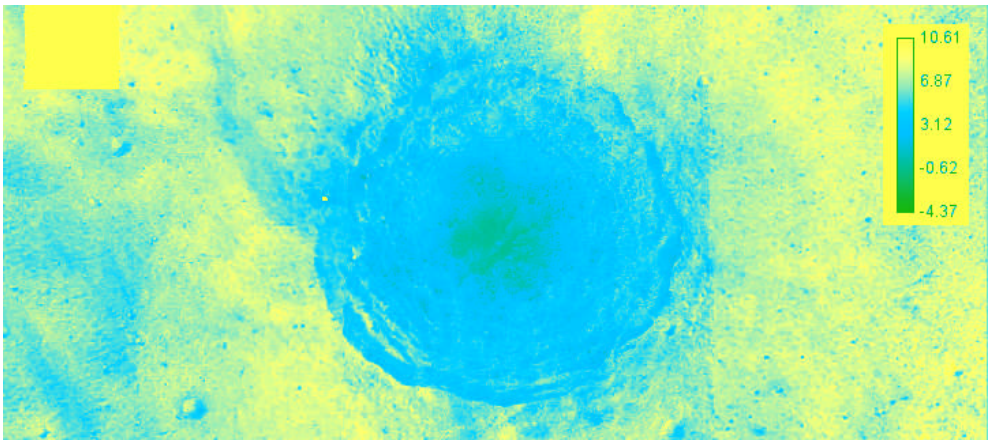

Fig. A4.3 f

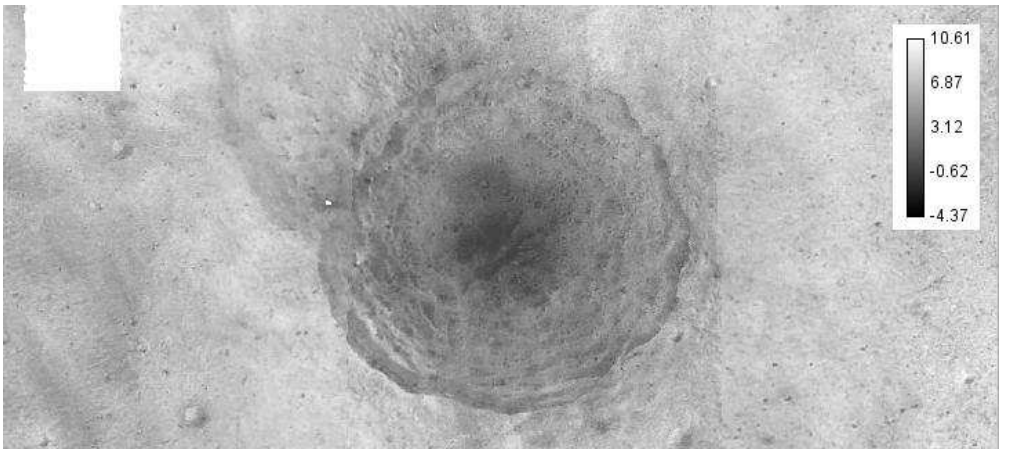

Fig. A4.3 g Total Iron

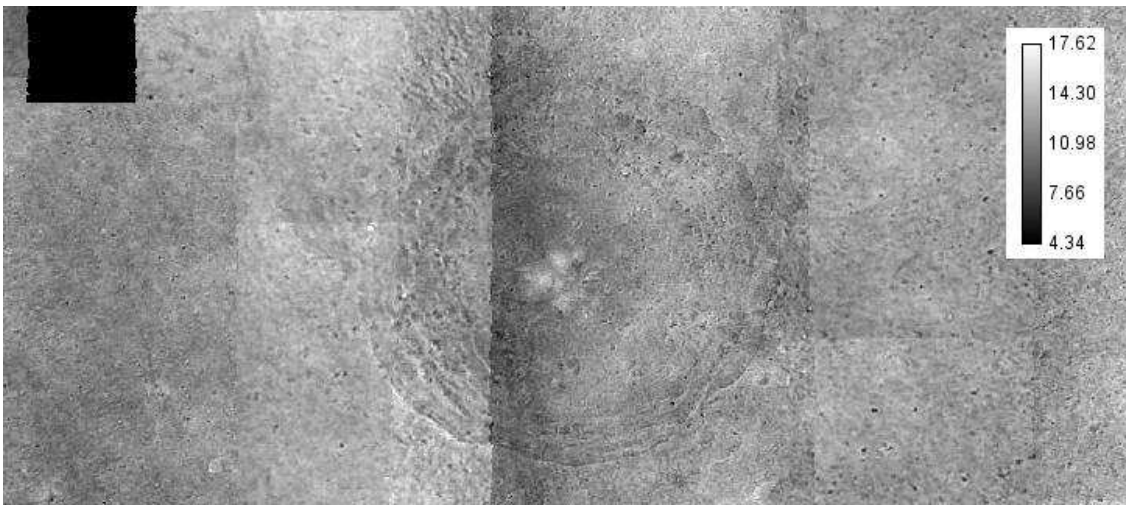

Fig.A4.3 h Total Iron Color Gradient

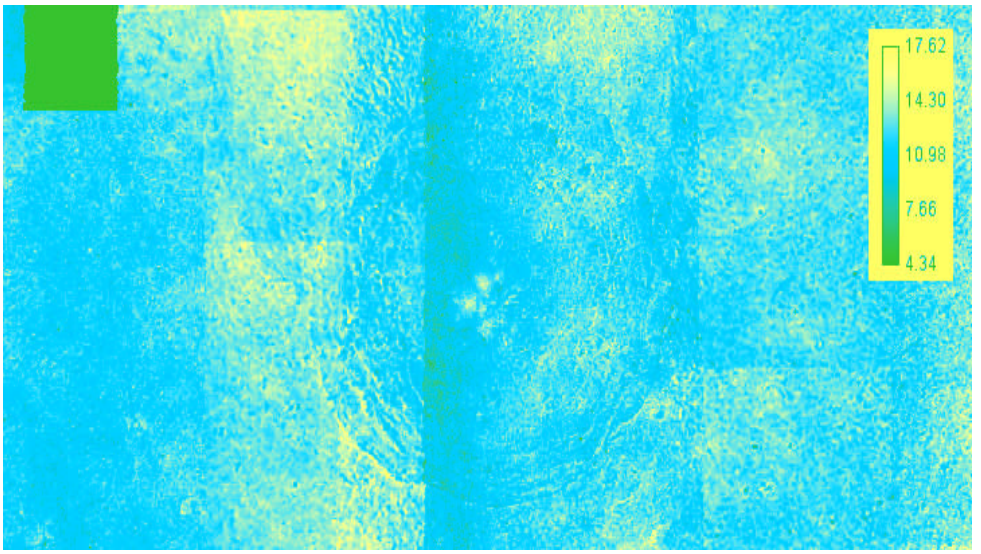

Fig. A4.3 i Absorption Trough Minimum Map

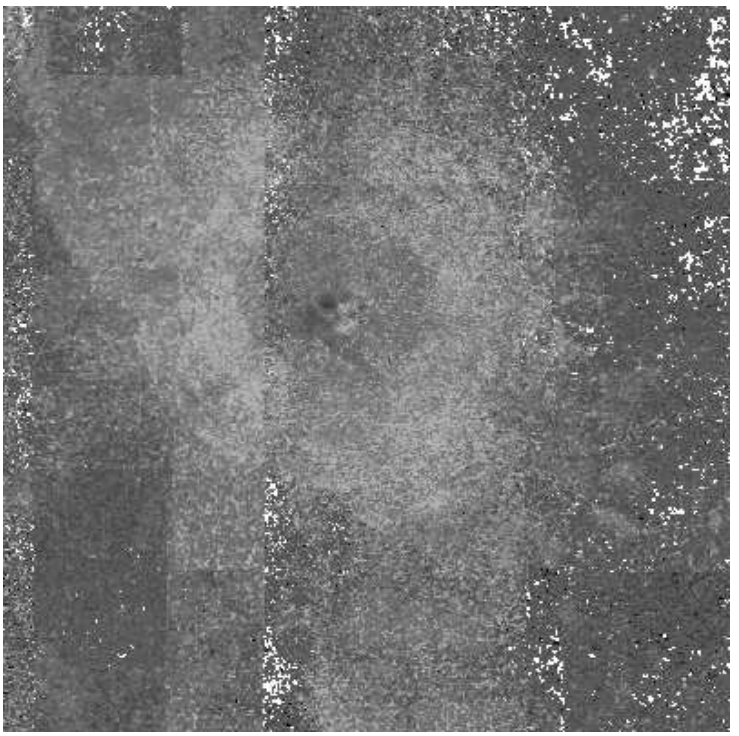

Fig. A4.3 j Absorption trough depth map

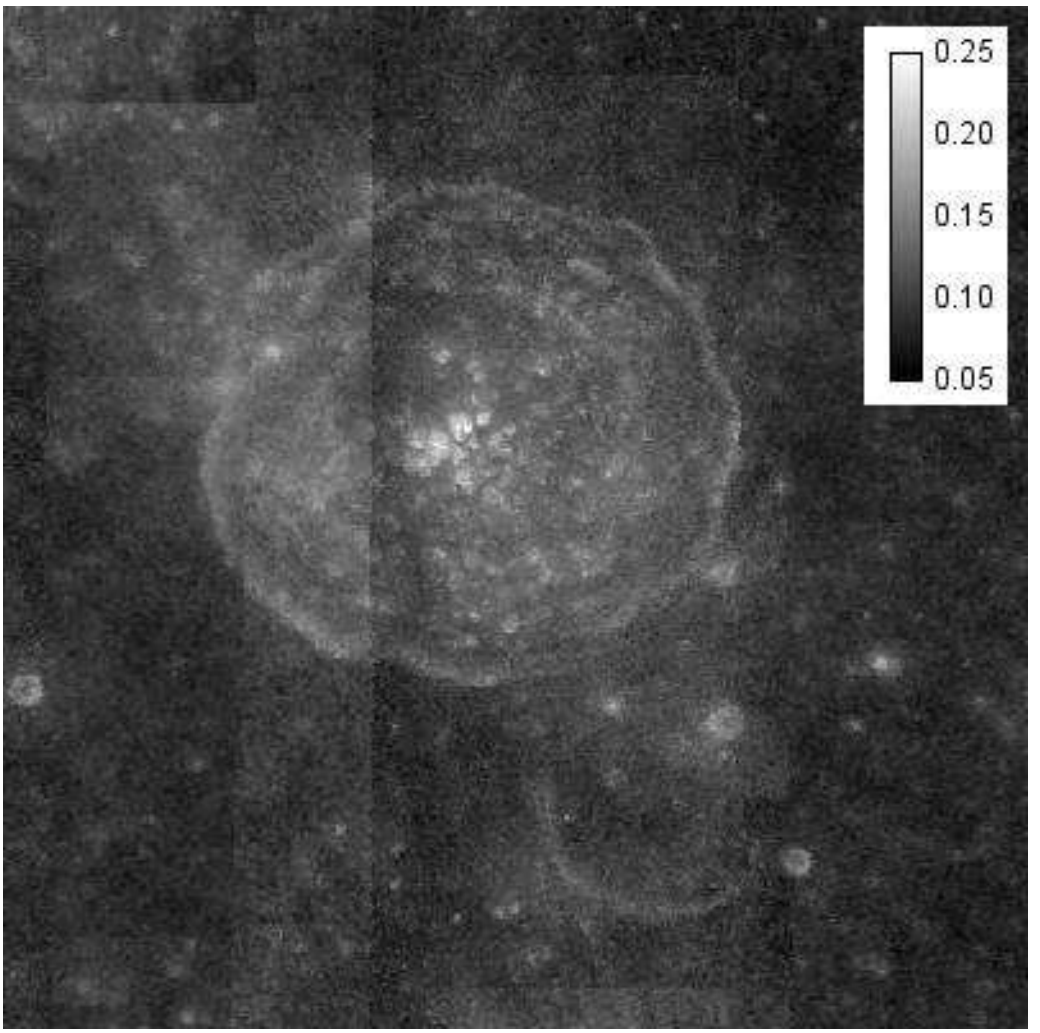

Fig A4.3 k FWHM map of Bullialdus

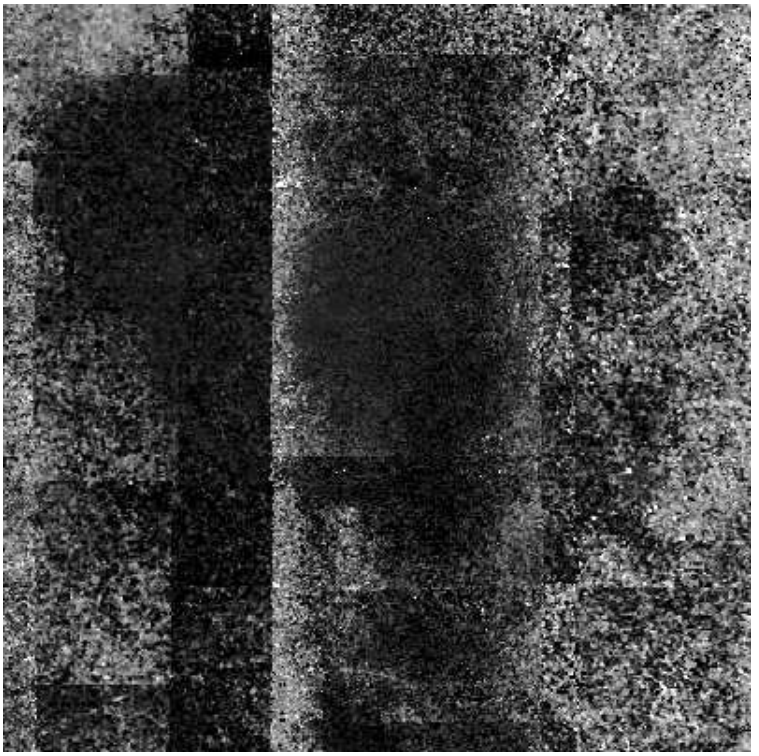

Fig A4.3 l Key to Geographic Features in Table A4.5-1

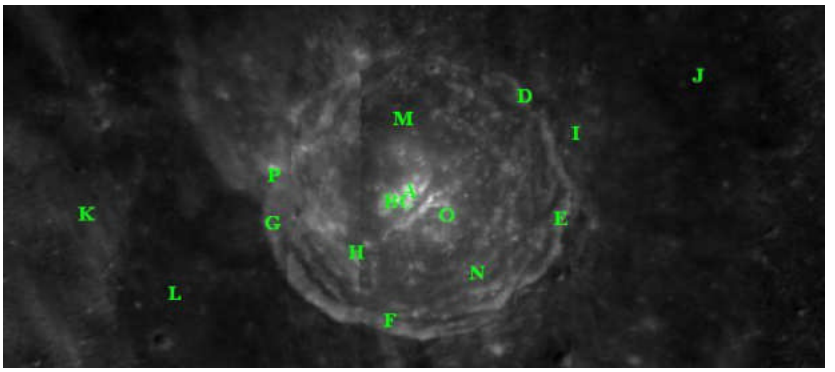

Table A4.3-1

Crater Feature (letter corresonds to labelled image)	Total Iron in wt% (note: method not valid for pyroplastic deposit assessment)	Band Center Estimate in microns	Absorption Depth % Corrected for Slope	% Depth Uncorrected for Slope	Continuum Slope scaled to tangency at 750nm
Central Peak (A)	13.5	0.930	39.9	.202	.692
Central Peak (B)	11.2	0.940	.354	.165	.661
Central Peak (C)	13.4	0.945	.400	.203	.690
NE Wall (D)	12.1	0.990	.268	.112	.547
East Wall (E)	11.1	0.985	.269	.112	.550
South Wall (F)	9.4	0.980	.224	.093	.458
West Wall (G)	13.2	0.985	.283	.109	.609
SW Crater Interior (H)	12.6	0.995	.275	.108	.585
Ejecta, East (I)	12.7	0.985	.239	.076	.570
Mare Nubium, East (J)	12.2	0.980	.195	.049	.512
Outside Crater (K)	11.2	0.985	.219	.068	.527
Mare Nubium, West (L)	12.4	0.980	.203	.056	.513
Crater Floor (M)	9.0	0.975	.246	.078	.588
Wall (N)	11.5	0.980	.268	.107	.563
Crater Interior (O)	11.3	0.975	.310	.121	.660
Small Crater on NW Rim (P)	13.0	0.970	.342	.143	.694

Fig. A4.3 m False Color Image
Red= Inverted Band Center; Green=2000/1500 nm; Blue=non-inverted Band Center

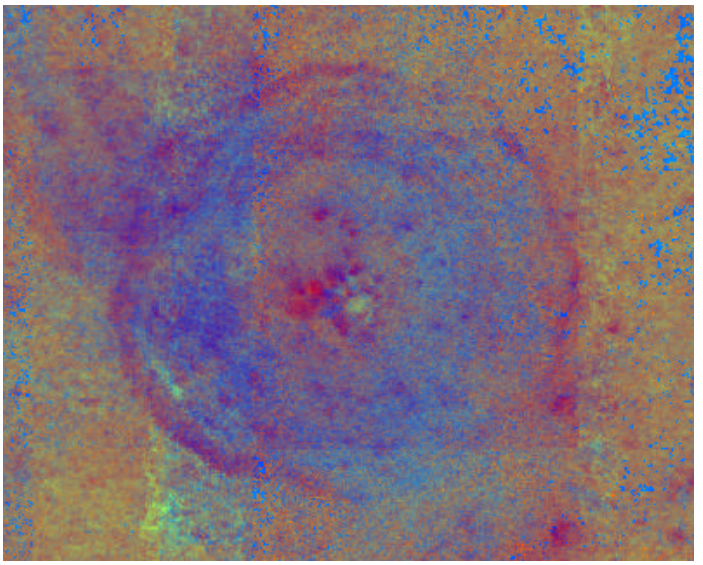

The false color map shown in Fig. A4.3 n below has height controlled by the band depth map while the false color overlay has the inverse of the band center map in the red channel, the FWHM map in the green channel, and the band center map in the blue channel.

Fig. A4.3 n

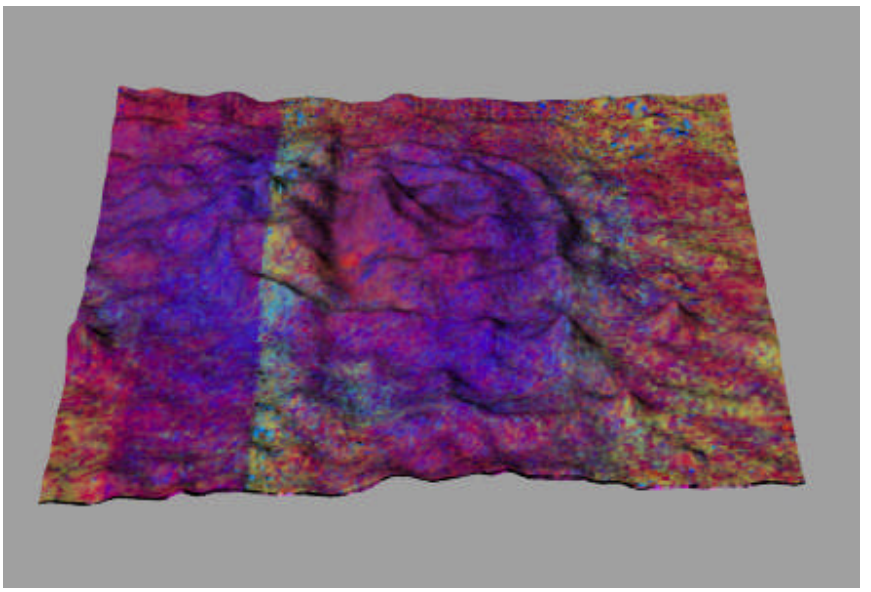

Appendix III: Additional Excel Map Studies

Dionysius

Fig. A 5.1

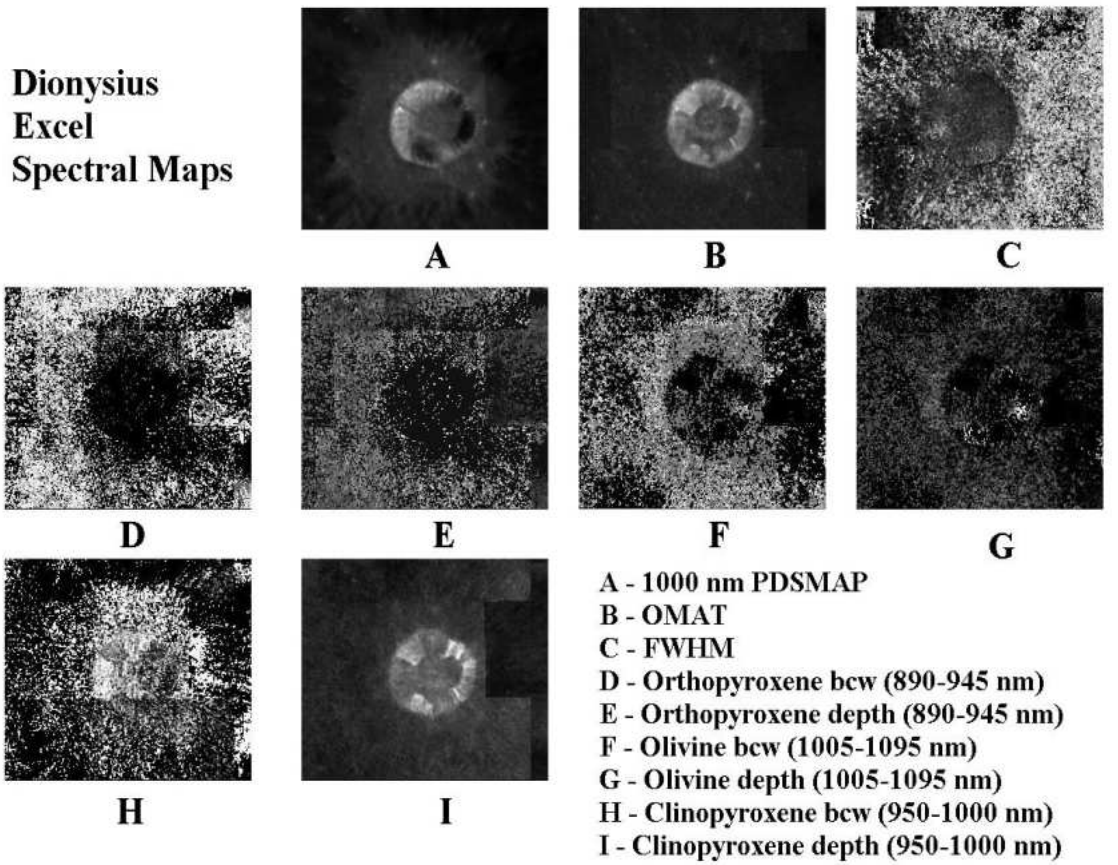

Fig. A 5.2

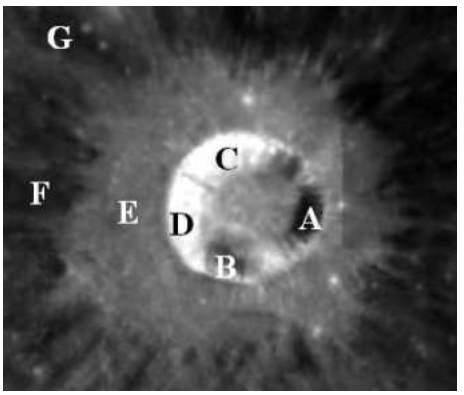

Table A 5.3 (refer to Fig A 5.2 above for locations of A thru G)

	Op bcw	Op depth	Cp bcw	Cp depth	Ol bcw	Ol depth	OMAT	FWHM
A	0.0	0.0	0.96	0.110	1.005 to 1.07	0.101	0.320	250
B	0.0	0.0	0.97	0.124	1.005 to 1.08	0.115	0.343	245
C	0.90	0.049	0.99	0.099	0.0	0.0	0.329	231
D	0.935	0.046	0.96	0.102	0.0	0.0	0.421	224
E	0.945	0.040	0.95	0.059	1.005 to 1.08	0.046	0.225	256
F	0.935	0.040	0.96	0.035	1.015 to 1.09	0.024	0.208	215
G	0.935	0.039	0.95	0.012	1.005 to 1.075	0.013	0.191	276

Interpretation:

The crater wall of Dionysius contains prominent basaltic patches rich in olivine and gabbro. These appear dark in the 1000 nm image. Other areas of the wall that appear brighter in the 1000 nm image contain mixtures of orthopyroxene and clinopyroxene. The proximal ejecta blanket of the crater shows a mixture of orthopyroxene, clinopyroxene and olivine with the orthopyroxene component being relatively greater than the other two components.

Stevinus
Fig. 5.4

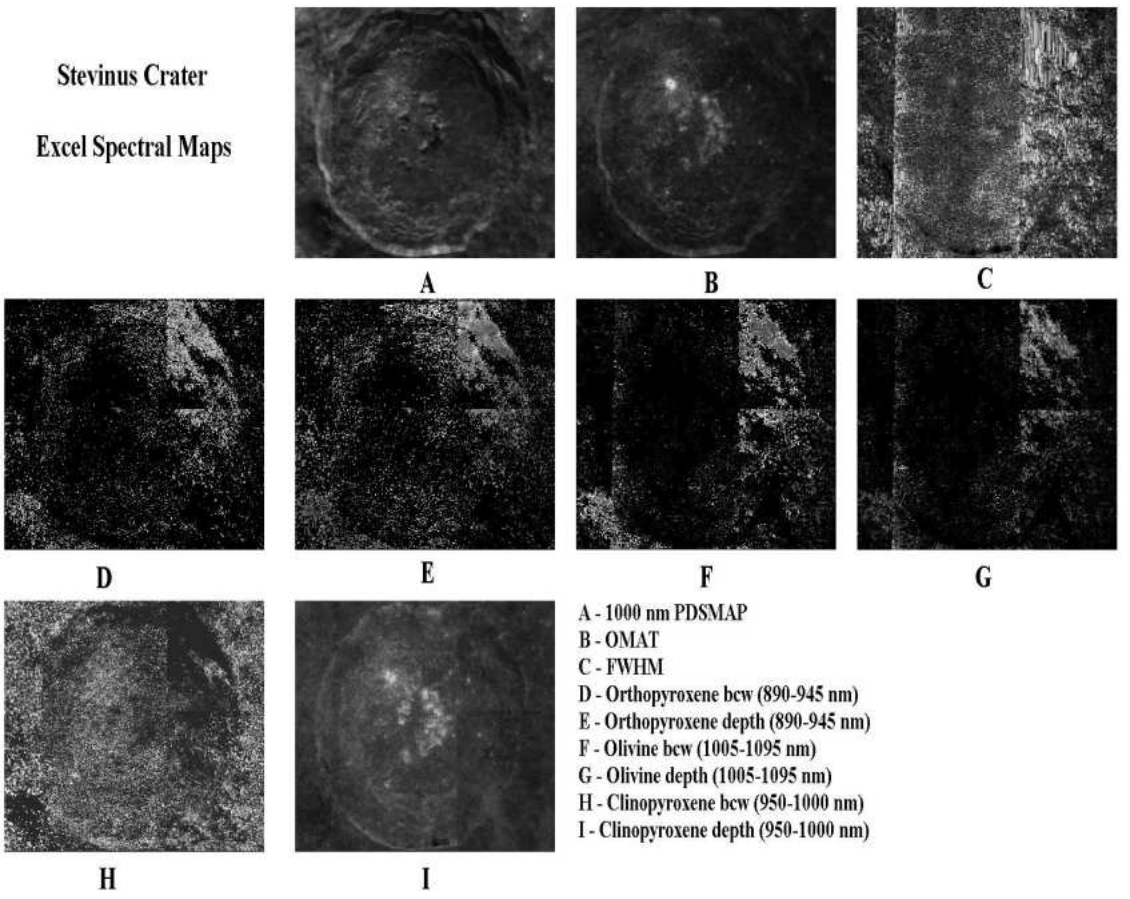

Fig. 5.5

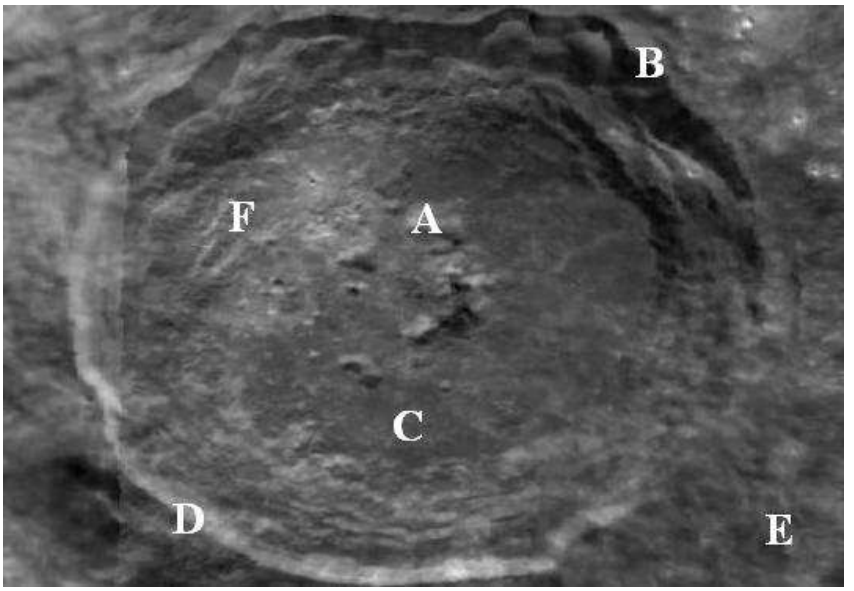

Table 5.6 (Refer to Fig. 5.5 for locations of A thru F)

	Op bcw	Op depth	Cp bcw	Cp depth	Ol bcw	Ol depth	OMAT	FWHM
A	0	0.0	0.97	0.188	0	0.0	0.458	245
B	0.935	0.060	0.97	0.085	1.02	0.0791	0.298	223
C	0.945	0.077	0.96	0.088	0	0.0	0.299	225
D	0	0.0	0.97	0.103	0	0.0	0.348	202
E	0.945	0.058	0.98	0.069	1.005 to 1.085	0.039	0.273	223
F	0.945	0.067	0.97	0.115	0	0.0	0.342	218

Interpretation:
The central peaks of Stevinus are mainly gabbroic. The northeast rim of the crater shows a prominent complex area of mixed orthopyroxene, clinopyroxene and olivine composition.

Straight Wall

Fig. 5.7

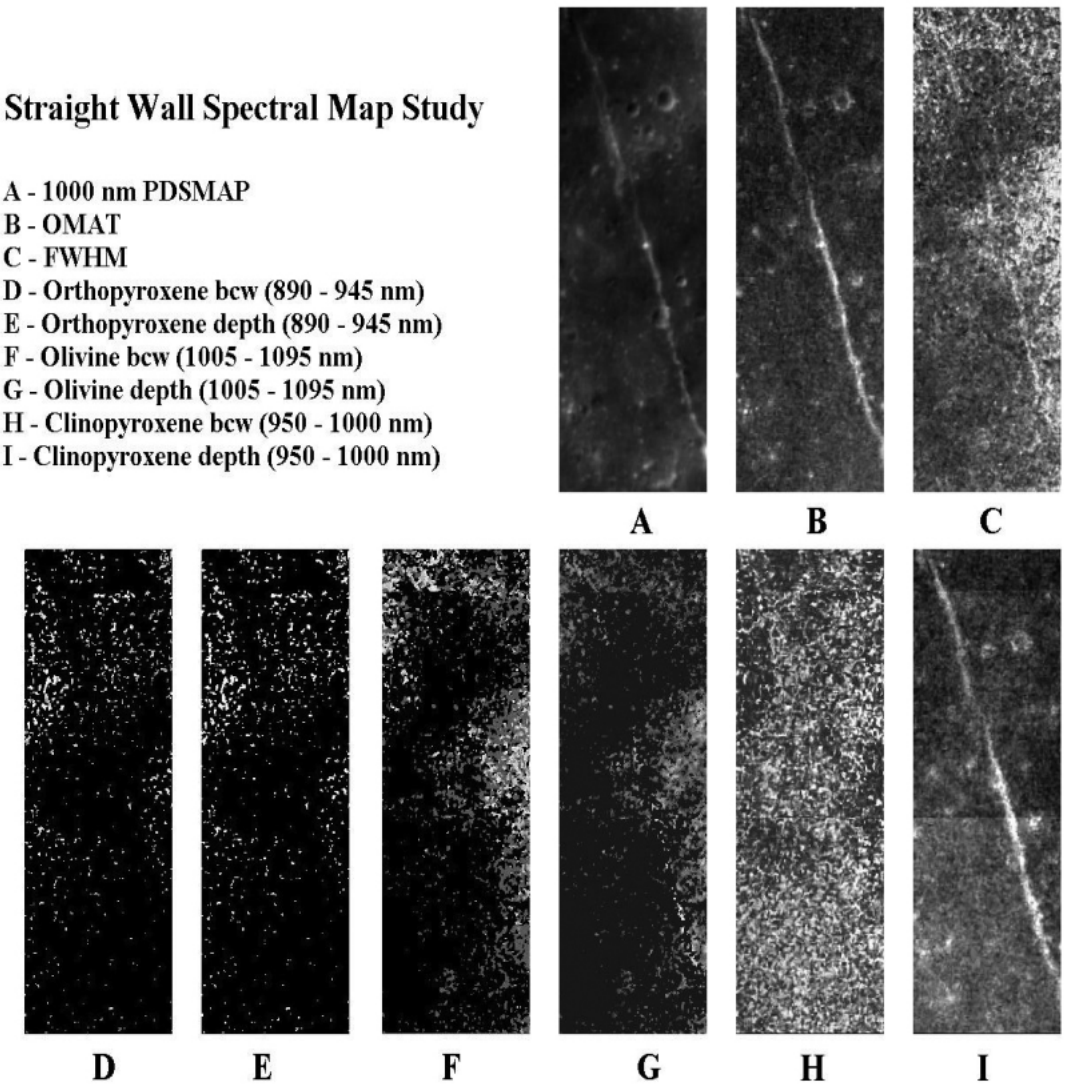

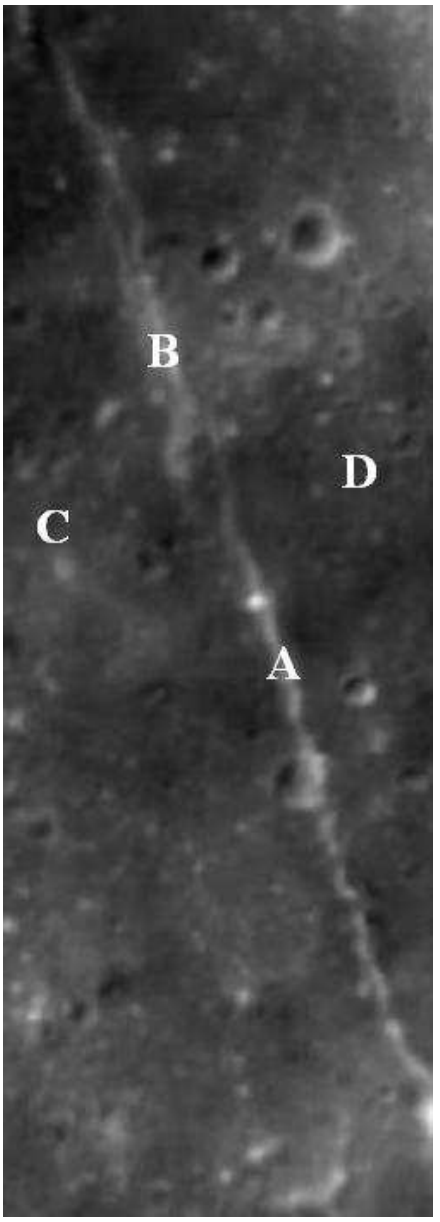

Fig. 5.7

Table 5.8 (see Fig. 5.7 for location of A thru D)

	Op bcw	Op depth	Cp bcw	Cp depth	Ol bcw	Ol depth	OMAT	FWHM
A	**0**	**0.0**	**0.980**	**0.128**	**1.005**	**0.064**	**0.311**	**270**
B	**0**	**0.0**	**0.980**	**0.105**	**0**	**0.0**	**0.259**	**219**
C	**0.935**	**0.074**	**0.980**	**0.066**	**1.005**	**0.03**	**0.219**	**210**
D	**0.94**	**0.085**	**0.980**	**0.060**	**1.05**	**0.76**	**0.217**	**268**

Interpretation:

The Straight Wall does not differ in composition from the adjacent mare, but the slope is less mature as seen in the OMAT map image. Consequently, the clinopyroxene and olivine band depth is increased within the slope. This is most likely due to landslides caused by occasional moonquakes since the slope has an inclination of about 20 degrees.